



**Synthesis and characterization of aromatic-PDMS  
segmented block copolymers and their shape-memory  
performance**

Journal:	<i>Polymer Chemistry</i>
Manuscript ID	PY-ART-05-2019-000682.R1
Article Type:	Paper
Date Submitted by the Author:	09-Aug-2019
Complete List of Authors:	Xu, Hongli; Delft University of Technology Bijleveld, Johan; Delft University of Technology, Aerospace Engineering Hegde, Maruti; University of North Carolina at Chapel Hill, Applied Physical Sciences Dingemans, Theo; University of North Carolina at Chapel Hill, Applied Physical Sciences



Journal name

PAPER

## Synthesis and characterization of aromatic-PDMS segmented block copolymers and their shape-memory performance

Hongli Xu,<sup>a,b</sup> Johan Bijleveld,<sup>b</sup> Maruti Hedge,<sup>c</sup> Theo Dingemans<sup>\*b,c</sup>

Received 00th January 20xx,  
Accepted 00th January 20xx

DOI: 10.1039/x0xx00000x

www.rsc.org/

In this paper we will describe the synthesis and properties of two series high molecular weight segmented block copolymers from all-aromatic amorphous (AM) or liquid crystal (LC) telechelic ester-based maleimide-functionalized oligomers ( $M_n = 5 \text{ kg}\cdot\text{mol}^{-1}$ ) and telechelic thiol-terminated poly(dimethylsiloxane) (PDMS,  $M_n = 1, 5 \text{ and } 10 \text{ kg}\cdot\text{mol}^{-1}$ ). The multiblock copolymers were prepared *via* highly efficient thiol-ene click chemistry, and have  $M_n$ s ranging from 22 to 58  $\text{kg}\cdot\text{mol}^{-1}$ . The segmented block copolymers prepared from mesogenic (LC) units show micro-phase separation and liquid crystallinity even with a PDMS content as high as 65 wt%. The AM5K-based series is completely amorphous. The multiblock copolymers with PDMS5K and 10K show two  $T_g$ s at  $\sim -120 \text{ }^\circ\text{C}$  and  $\sim 120 \text{ }^\circ\text{C}$ , respectively, implying the presence of a (micro)phase separated system. The multiblock copolymer prepared from AM5K and PDMS1K displays excellent stress-strain behavior at  $25 \text{ }^\circ\text{C}$ , with a tensile strength of 123.6 MPa, an elastic modulus of 3.4 GPa, an elongation at break of 31.2% and toughness of  $30.7 \text{ MJ}\cdot\text{m}^{-3}$ . The LC5K based multiblock copolymer films exhibit poor stress-strain behavior, which is the result of a higher degree of phase separation and low phase intermixing, as confirmed by TEM measurements. The shape memory properties of the PDMS-containing segmented block copolymers in the temperature range of  $-150 \text{ to } 150 \text{ }^\circ\text{C}$  were tested using a rheometer in torsion mode. The glass transitions originating from the rigid aromatic blocks and flexible PDMS blocks were used as the reversible switches for designing  $T_g$ -based dual- and triple-shape memory polymer films. The AM5K-*b*-PDMS1K and LC5K-*b*-PDMS1K multiblock copolymers show dual-shape memory behavior in the temperature range of  $20\text{--}150 \text{ }^\circ\text{C}$ . The PDMS5K based analogs show triple shape-memory behavior in the temperature range of  $-150\text{--}150 \text{ }^\circ\text{C}$ .

### Introduction

Segmented block copolymers are an important class of engineering plastics because they offer outstanding mechanical performance in combination with thermoplastic processing. Examples include polyurethane based thermoplastic elastomers (TPEs), polyester-based TPEs, and polyamide-based TPEs.<sup>1</sup> Typically, this type of block copolymer is composed of at least one rigid block and one soft block, which are covalently connected. The rigid block acts as a (temporary) physical crosslink unit and the soft segment provides the segmented block copolymer with ductility. Segmented block copolymers based on high-performance polymer building blocks have been reported as well, including amorphous, semi-crystalline or liquid crystalline (LC) high-performance polymers.<sup>2</sup> Pospiech *et al.* reported on the phase behavior of segmented block copolymers containing segments with different degrees of flexibility and different molecular weights, including poly(tetramethylene

oxide)-polysulfone multiblock copolymers and polysulfone-semifluorinated polyester multiblock copolymers.<sup>3</sup>

When using an aromatic LCP as the rigid-block, the resulting block copolymers may exhibit liquid crystallinity, depending on the composition of the second (soft) block. LC multiblock copolyesters of oxybenzoate and ethylene terephthalate (POB-PET) were prepared *via* a direct condensation reaction of poly(hydroxybenzoic acid) (PHBA), acetoxybenzoic acid and poly(ethylene terephthalate) and studied by Ho *et al.*<sup>4</sup> Only 20 mol% of POB is needed to form a nematic phase in these multiblock POB-PET as opposed to a minimum of 40 mol% POB that is required to form a nematic phase in random POB-PET. Polyethersulfone-aramid *i.e.* Polyethersulfone-aromatic polyamide block copolymers were synthesized from a diamine-terminated polyethersulfone oligomer, aromatic diamines, and aromatic dicarboxylic acid chlorides using a low-temperature solution polycondensation.<sup>5</sup> With the introduction of an aramid (aromatic polyamide) into the polyethersulfone backbone, the glass transition temperatures and mechanical properties of the block copolymers were greater. In contrast to most block copolymers, microphase separation did not occur in this multiblock copolymer system. Smectic multiblock copolymers containing unsaturated polyethers and aromatic poly(ethersulfone)s were condensed in the presence of a phase transfer catalyst by Percec *et al.*<sup>6-8</sup> The authors studied the reaction conditions and thermal properties of the multiblock copolymers. They concluded that these multiblock copolymers

<sup>a</sup> School of Innovation and Entrepreneurship, Southern University of Science and Technology, 518055 Shenzhen, China.

<sup>b</sup> Faculty of Aerospace Engineering, Delft University of Technology, Kluyverweg 1, 2629 HS Delft, The Netherlands.

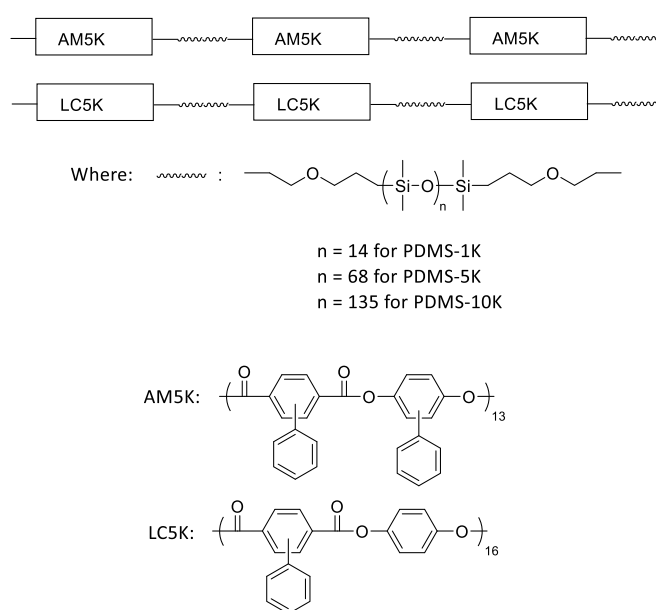
<sup>c</sup> Department of Applied Physical Sciences, University of North Carolina at Chapel Hill, Murray Hall 1113, Chapel Hill, North Carolina 27599-3050, United States.

† Electronic Supplementary Information (ESI) available. See DOI: 10.1039/x0xx00000x

show no phase separation because only one  $T_g$  was detected by DSC. Multiblock copolymers with poly(tetramethylene glycol) (PTMG) spacers of different length and 4,4'-(terephthaloyldioxy) dibenzoyl units were reported by Mitrach *et al.*<sup>9</sup> Nematic textures were observed for block copolymers with spacer molecular weights up to 650 g·mol<sup>-1</sup>. Above the spacer molecular weights of 1000 g·mol<sup>-1</sup>, the polymers tend to crystallize into different polymorphs.

When incorporating a flexible polydimethylsiloxane block ( $T_g \sim -125$  °C) into a segmented block copolymer formulation, several improvements in properties can be noted with respect to processability and toughness.<sup>10</sup> Several different types of dianhydrides and diamines, including 4,4'-oxydiphthalic anhydride (ODPA), bisphenol-A-dianhydride (BPADA), 2,2-bis(4-[4-aminophenoxy]phenyl)propane (BAPP), 4,4-(bis(3-trifluoromethyl-*p*-aminobiphenyl ether) biphenyl have been utilized as the hard block to prepare segmented multiblock poly(imidesiloxane)s.<sup>10-17</sup> Fluorinated poly(imide-siloxane)s show  $T_g$ s of 107 – 203 °C, and a film tensile strength at break of 24–75 MPa ( $\epsilon = 24$ –144%), depending on the siloxane loading.<sup>12</sup> Multiblock copolymers based on PDMS and aromatic amides were first introduced by Kajiyama *et al.*<sup>18</sup> The segmented multiblock copolymers behave as rubber-toughened aramid plastics, having tensile strength and fracture elongation of 60 MPa and 9%, respectively at low PDMS loading. At higher PDMS concentrations, the resulting block copolymers are analogous to TPEs, showing tensile strength and fracture elongation of up to 6 MPa and 140%, respectively.<sup>18</sup> Similar mechanical behavior, was reported by Cureton *et al.* on a series of hexafluoroisopropylidene bisphenol poly(arylene ether sulfone)–PDMS block copolymers, where a higher concentration of soft blocks resulted in lower tensile strengths (8 – 24 MPa).<sup>19</sup> In all reported cases, none of the polymers exhibit a tensile strength exceeding 80 MPa. The mechanical properties of the block copolymers appear to be compromised by the soft domains and weakened by PDMS induced phase separation.<sup>3</sup>

In this paper, a facile approach towards the preparation of segmented block copolymers from bis-maleimide functionalized all-aromatic telechelic oligomers and thiol-terminated PDMS segments *via* a highly efficient base-catalyzed thiol-ene click reaction is presented.<sup>20</sup> Compared to other alkene candidates like (meth)acrylates and fumarate esters, maleimides are intrinsically activated substrates for base catalyzed thiol-ene reactions. Due to the presence of two activating carbonyl groups in a *cis*-conformation coupled with ring-strain/bond angle distortion, the C=C bond in maleimides is very reactive and thiol-ene reactions can take place extremely fast.<sup>21</sup> However, a typical thiol-ene click reaction has to take place in solution, making this highly efficient reaction not widely used in preparing high-performance block copolymers, due to the very limited solubility of aromatic segments. To the best of our knowledge, this is the first example of multiblock copolymers prepared from all-aromatic segments *via* thiol-ene click chemistry. The molecular composition of the multiblock copolymers is shown in Scheme 1. The fact that both aromatic blocks, *i.e.* AM5K and LC5K, have very similar



**Scheme 1.** Molecular composition of the aromatic–PDMS-based  $(AB)_n$ -multiblock copolymers. The aromatic block ( $M_n = 5,000$  g/mol or 5K) is either amorphous (AM) or liquid crystalline (LC) and the PDMS block is 1,000 (1K), 5,000 (5K) or 10,000 (10K) g/mol.

backbone structures and at the same time exhibit distinct different phase behavior (amorphous vs LC) makes them perfect candidates for studying the effect of phase behavior (amorphous vs nematic) on the thermomechanical properties of thin films. The morphological, thermal and mechanical properties of the multiblock amorphous (AM) and LC copolymers are explored as function of different PDMS block lengths, *i.e.* 1, 5 and 10 kg/mol. Because of the large difference in  $T_g$  between the hard aromatic and soft PDMS blocks and the nanophase separation originating from the incompatibility of the two different blocks, we have also investigated the shape-memory characteristics of this new family of segmented block copolymers.

## Results and discussion

### Synthesis of the maleimide end-group and monomers

All monomers, thiol-terminated PDMS oligomers and maleimide-terminated aromatic polyesters were prepared using known procedures. The N-(4-hydroxyphenyl) maleimide (HPM) end-group was synthesized by condensing *p*-aminophenol with maleic anhydride.<sup>22-25</sup> Characterization, including NMR and MS, confirmed the molecular structure and purity of the target compound.

The synthesis of phenylterephthaloyl chloride (PTPC) has been reported in the literature by Land *et al.* with an overall yield of less than 46%.<sup>26</sup> The synthesis consists of three steps: first, 2,5-dimethylbiphenyl was synthesized; next, the methyl groups were oxidized with  $KMnO_4$ , and finally, the dicarboxylic acid was converted to the diacid chloride (PTPC) by using thionyl chloride, catalysed by DMF. To increase the yield and decrease

the formation of side products, a modified procedure was developed. Here, 2,5-dimethylbiphenyl was prepared by phenylation of 2-bromo-1,4-dimethylbenzene using Suzuki coupling conditions. The yield was found to be nearly quantitative, which is comparable to similar reports in the literature.<sup>27</sup> The obtained 2,5-dimethylbiphenyl was oxidized with  $\text{KMnO}_4$ , in moderate yields with pyridine as a phase transfer agent. The resulting diacid was converted to the diacid chloride under reflux with thionyl chloride. The overall yield was 76%, which is significantly higher than the 46% yield reported by Land *et al.*<sup>26</sup> Characterization using NMR and MS confirmed the structure and purity of PTPC.

#### Synthesis and molecular weight characterization of the AM5K and LC5K oligomers

The maleimide functionalized oligomers were synthesized *via* a standard solution polycondensation technique in anhydrous 1,1,2,2-tetrachloroethane (TCE).<sup>28, 29</sup> The polymerizations were straightforward and no evidence for premature cross-linking of the maleimide end-group, such as gelation or precipitation, was observed under the reaction conditions used. The obtained oligomers were analysed by  $^1\text{H}$  NMR and the proton assignment of the oligomers are shown in Figure S1.

The AM5K sample was analyzed using GPC and the molecular weight information is summarized in Table 1. The LC5K sample is not soluble in the GPC eluent (THF), and could only be characterized by viscometry. The AM5K sample showed a unimodal molecular weight distribution and PDI of  $\sim 2$ , which is consistent with step-growth polymerization. The  $M_n$  values from GPC deviate from the theoretical values. This can be understood when one considers the fact that polystyrene, a random coil polymer, was used as the internal standard for the GPC measurements. The molecular weights calculated using the Mark-Houwink-Sakurada equation as well as the inherent viscosity of the 5K oligomers are presented in Table 1. Generally, the molecular weight value from viscometry measurements agrees with the calculated  $M_n$  value. We have performed quantitative  $^{13}\text{C}$  NMR experiments (Figure S2) and the calculated  $M_n$  results are summarized in Table 1 as well. The calculated  $M_n$ s of the oligomers are in close agreement with the targeted molecular weights and viscometry analysis.

#### Synthesis and molecular weight characterization of the thiol-terminated PDMS oligomers

Sample	$M_{n, \text{theo}}^1$	$M_{n, \text{GPC}}(\text{PDI})^2$	$M_v^3$	$\eta_{\text{inh}}^4$	$M_{n, \text{NMR}}^5$
AM5K	5.0	11 (2.0)	5.5 <sup>7</sup>	0.52	4.9
LC5K	5.0	– <sup>6</sup>	7.1 <sup>8</sup>	0.70	5.3

<sup>1</sup> Theoretical molecular weight (in  $\text{kg}\cdot\text{mol}^{-1}$ ) calculated by Carothers equation. <sup>2</sup>  $M_n$  (in  $\text{kg}\cdot\text{mol}^{-1}$ ) and PDI from GPC measurement, was performed using THF as eluent and polystyrene as internal standard. <sup>3</sup>  $M_v$  (in  $\text{kg}\cdot\text{mol}^{-1}$ ) calculated using the Mark-Houwink-Sakurada equation (equation 4, experimental section). <sup>4</sup> Inherent viscosity (in  $\text{dL}\cdot\text{g}^{-1}$ ) obtained from viscometry measurements. <sup>5</sup>  $M_n$  (in  $\text{kg}\cdot\text{mol}^{-1}$ ) calculated from quantitative  $^{13}\text{C}$  NMR results. <sup>6</sup> Could not be determined due to limited solubility in THF at room temperature. <sup>7</sup> Viscometry measurement of AM5K was performed in 1,4-dioxane at a concentration of  $0.5 \text{ g}\cdot\text{dL}^{-1}$  at  $21^\circ\text{C}$ . <sup>8</sup> Viscometry measurement of LC5K was performed in TCE at a concentration of  $0.5 \text{ g}\cdot\text{dL}^{-1}$  at  $21^\circ\text{C}$ .

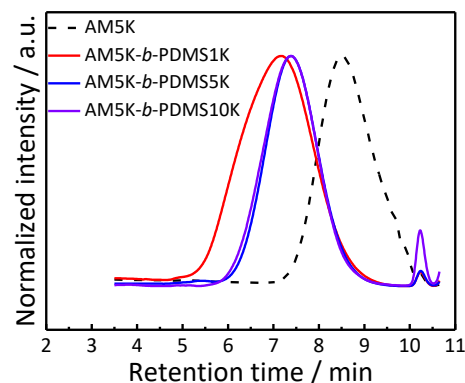


Fig. 1. GPC curves obtained for the soluble (THF) AM5K oligomer and AM5K-*b*-PDMS1K, -5K and -10K block copolymers. All curves are normalized to maximum intensity. Note that the LC-series could not be analyzed using GPC because of the limited solubility in THF.

The thiol-functionalized PDMS oligomers were synthesized starting from commercial telechelic hydroxyl-functionalized PDMS with molecular weights of 1, 5 and 10  $\text{kg}\cdot\text{mol}^{-1}$ , respectively. The synthetic procedure was based on a procedure published by van de Berg *et al.*<sup>30</sup>, however, a modified procedure was developed, with the aim to increase the overall yield.

The number average molecular weights ( $M_n$ s) for the PDMS-SH oligomers were calculated based on the proton signals of the end-groups and in the main-chain of PDMS and the results are summarized in Table 2. The proton NMR spectra of PDMS1K-SH and PDMS1K-OH is available in the SI as an example (Figure S3) together with the relevant molecular weight calculations. The molecular weights for the 5K and 10K oligomers match the target molecular weights quite closely, only the 1K oligomer is somewhat higher. This is because the commercial source of PDMS1K-OH has an  $M_n$  of  $1.4 \text{ kg}\cdot\text{mol}^{-1}$ . We observe a slight increase in molecular weight and polydispersity going from the hydroxyl terminated oligomer to the thiol terminated oligomer as observed by GPC (Figure S4). For example, the number average molecular weights before and after end-group modification of PDMS1K-OH and PDMS1K-SH are 1.8K (PDI of

Table 2. Molecular weights of the PDMS oligomers as determined by GPC,  $^1\text{H}$  NMR and viscometry.

Sample	$M_{n, \text{GPC}}^1$	$M_w, \text{GPC}^2$	$\text{PDI}^1$	$M_{n, \text{NMR}}^2$	$\eta_{\text{inh}}^3$
PDMS1K-OH	1.8	2.5	1.4	1.4	0.030
PDMS5K-OH	6.0	9.0	1.4	4.8	0.059
PDMS10K-OH	13	20	1.5	11.2	– <sup>4</sup>
PDMS1K-SH	2.2	3.4	1.5	1.53	0.032
PDMS5K-SH	7.8	12	1.4	5.03	0.063
PDMS10K-SH	13	18	1.4	11.6	– <sup>4</sup>

<sup>1</sup> Molecular weights (in  $\text{kg}\cdot\text{mol}^{-1}$ ) and polydispersity index was measured by GPC with THF as eluent at a flow rate of  $1 \text{ mL}\cdot\text{min}^{-1}$ , calibrated using monodisperse polystyrene standards. <sup>2</sup> Molecular weights (in  $\text{kg}\cdot\text{mol}^{-1}$ ) were calculated from  $^1\text{H}$  NMR results (measured in  $\text{CDCl}_3$  at room temperature). <sup>3</sup> Inherent viscosities (in  $\text{dL}\cdot\text{g}^{-1}$ ) were measured by capillary viscometer using TCE at a concentration of  $0.5 \text{ g}\cdot\text{dL}^{-1}$  at  $21^\circ\text{C}$ . <sup>4</sup> Not determined due to limited solubility in TCE.

1.4) and 2.2K (PDI of 1.5)  $\text{kg}\cdot\text{mol}^{-1}$ , respectively, relative to polystyrene standards. This slight increase was observed for all PDMS oligomers resulting from disulfide formation as confirmed by NMR experiments, see Figure S3 and S4. The resulting  $M_n$ s,  $M_w$ s, as well as PDI obtained from GPC experiments are listed in Table 2, and are found to be consistently higher than the NMR results, due to the calibration of the GPC with polystyrene, resulting in an overestimation of the  $M_n$ .

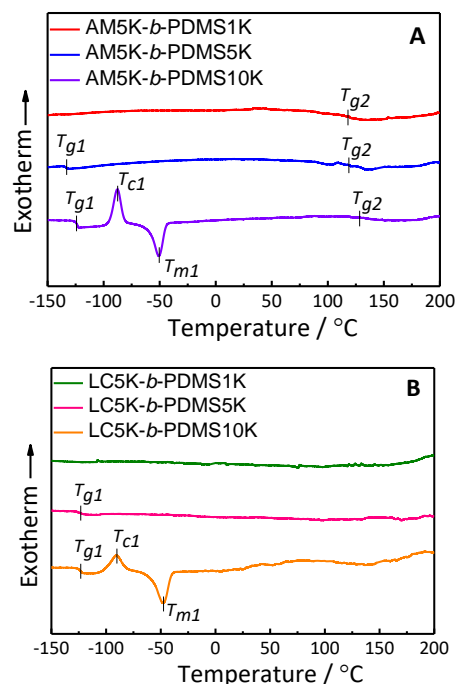
#### Synthesis and molecular weight characterization of the segmented block copolymers

Table 3 lists the molecular weights and PDMS content of the block copolymers as calculated by  $^1\text{H}$  NMR and as determined by GPC. The NMR spectra of AM5K-*b*-PDMS1K and its constituent components is shown in the SI (Figure S5) together with the detailed calculations. The GPC traces of the soluble AM5K-*b*-PDMS block copolymers are shown in Figure 1. The LC-based block copolymers are not soluble in THF and therefore could not be analysed using GPC. The PDMS content as determined by  $^1\text{H}$  NMR is close to the theoretical value, confirming the efficiency of the thiol-ene click chemistry. The results from the different techniques show a similar trend and have the same order of magnitude. As expected, the polydispersity of the block copolymers is slightly higher than that of the oligomers, which can be attributed to the polydispersity of the starting materials. If we take  $M_n$  as calculated from NMR experiments ( $M_n$  ranges from 22–58  $\text{kg}/\text{mol}$ ), we may conclude that high molecular polymer can indeed be prepared using click chemistry.

The inherent viscosity of both the block copolymers and oligomers was measured in TCE. Since the block copolymers have different molecular compositions, a direct comparison of their inherent viscosity cannot be made. A higher inherent viscosity of different polymers does not necessarily imply a higher molecular weight.

#### Thermogravimetric analysis (TGA)

The thermal stability of the segmented block copolymers was evaluated using dynamic thermogravimetric analysis (TGA) at a heating rate of  $10\text{ }^\circ\text{C}\cdot\text{min}^{-1}$ . The TGA thermograms of the as-made block copolymers are shown in Figure S6, and  $T_d^{5\%}$  and char yields are



**Fig. 2.** DSC curves of the  $(\text{AB})_n$  block copolymers. In the graphs the glass transitions ( $T_g$ s) are marked with a vertical bar. **A-** AM5K-*b*-PDMS series; **B-** LC5K-*b*-PDMS series. All data was collected from the first heating cycle at a heating rate of  $40\text{ }^\circ\text{C}\cdot\text{min}^{-1}$  of as-prepared samples under a helium atmosphere. The graphs are offset for clarity.

summarized in Table 4. When increasing the length of the PDMS segments the  $T_d^{5\%}$  of the block copolymers shows a dramatic increase. This is reflected in both series where the polymers with short PDMS blocks (PDMS 1K) will decompose at lower temperatures ( $T_d^{5\%} \sim 346\text{ }^\circ\text{C}$ ) and polymers with large PDMS blocks (PDMS 10K) will show high decomposition temperatures ( $T_d^{5\%} \sim 423\text{ }^\circ\text{C}$ ). The thermal stability of both block copolymer series is excellent and in line with what is observed for other high-performance polymers.

#### Differential scanning calorimetry analysis (DSC)

The thermal transitions were investigated using DSC experiments and the DSC traces of the as-made block copolymers are shown in Figure 2 and the results are

**Table 3.** Molecular weight results of  $(\text{AB})_n$  multiblock copolymers.

Samples	GPC results <sup>1</sup>			$M_n(\text{kg}\cdot\text{mol}^{-1}, \text{NMR})^3$	$\eta_{inh}$ ( $\text{dL}\cdot\text{g}^{-1}$ ) <sup>4</sup>	PDMS content (theoretical) <sup>5</sup>	PDMS content (NMR) <sup>6</sup>
	$M_n(\text{kg}\cdot\text{mol}^{-1})$	$M_w(\text{kg}\cdot\text{mol}^{-1})$	PDI				
AM5K- <i>b</i> -PDMS1K	93	417	4.4	32	1.74	22%	25%
AM5K- <i>b</i> -PDMS5K	72	168	2.3	46	1.71	51%	52%
AM5K- <i>b</i> -PDMS10K	77	189	2.5	58	0.97	69%	70%
LC5K- <i>b</i> -PDMS1K	– <sup>2</sup>	–	–	22	1.20	22%	26%
LC5K- <i>b</i> -PDMS5K	– <sup>2</sup>	–	–	37	0.96	49%	46%
LC5K- <i>b</i> -PDMS10K	– <sup>2</sup>	–	–	44	0.56	66%	65%

<sup>1</sup> Molecular weight and polydispersity index was measured by GPC with THF eluent at a flow rate of  $1\text{ mL}\cdot\text{min}^{-1}$ , calibrated using polystyrene standards. <sup>2</sup> Not determined due to limited solubility in THF. <sup>3</sup> Molecular weights were calculated from  $^1\text{H}$  NMR results (details can be found in the supporting information). <sup>4</sup> Inherent viscosities were measured by capillary viscometer in TCE at a concentration of  $0.5\text{ g}\cdot\text{dL}^{-1}$  at  $21\text{ }^\circ\text{C}$ . <sup>5</sup> PDMS content was calculated from feed ratios. <sup>6</sup> PDMS content was calculated from  $^1\text{H}$  NMR experiments.



summarized in Table 4. The PDMS blocks exhibit  $T_g$ s at approximately  $-120\text{ }^\circ\text{C}$  and are clearly discernible in AM5K-*b*-PDMS5K and AM5K-*b*-PDMS10K. In addition to the  $T_g$  associated with the PDMS block, a  $T_g$  of approximately  $120\text{ }^\circ\text{C}$  associated with the aromatic AM5K block can clearly be seen. The presence of two  $T_g$ s is a strong indicator of a (micro)phase separated block copolymer.<sup>3</sup> In contrast, the DSC curve of AM5K-*b*-PDMS1K shows only one  $T_g$ , which is the result of the short PDMS segments.

Similarly, the  $T_g$ s of the PDMS blocks are clearly discernable in the LC5K-*b*-PDMS5K and LC5K-*b*-PDMS10K DSC curves, while that of the LC5K-*b*-PDMS1K shows no clear  $T_g$ . The glass transition of the aromatic LC block cannot be observed. The DSC curves of the block copolymers of both AM5K-*b*-PDMS10K and LC5K-*b*-PDMS10K show crystallization and melting peaks of the PDMS blocks at  $-82\text{ }^\circ\text{C}$  ( $T_c$ ) and  $-48\text{ }^\circ\text{C}$  ( $T_m$ ). PDMS crystallization has also been reported in other PDMS-based segmented block copolymers by Feng *et al.*<sup>31</sup> The crystal to nematic transition ( $T_{K-N}$ ) and isotropic transition ( $T_{N-I}$ ) of LC block copolymers are hardly observed in DSC curves.

#### Hot stage optical microscopy analysis (OM)

As reported previously, the high molecular weight LC polymer based on PTPC and HQ shows a thermotropic nematic phase in the temperature range of  $287\text{--}369\text{ }^\circ\text{C}$ .<sup>32</sup> The LC behavior of the block copolymers was investigated with respect to the molecular weight of PDMS blocks using polarized optical microscope with crossed polarizers. With the introduction of PDMS blocks, the liquid crystalline window was maintained and the crystal to nematic transition temperatures ( $T_{K-N}$ ) of LC5K-*b*-PDMS1K, 5K and 10K are hardly affected and are all around  $270\text{ }^\circ\text{C}$ . Upon further heating, the block copolymers show a nematic to isotropic transition ( $T_{N-I}$ ) at  $390\text{ }^\circ\text{C}$ , which is close to the  $T_d^{5\%}$  and effectively resulting in a nematic window of  $120\text{ }^\circ\text{C}$ . Polymerizing the LC5K oligomer with PDMS results in a broadening of the nematic window by  $\sim 40\text{ }^\circ\text{C}$ , which is believed to be due to an increase in chain mobility imparted by the PDMS block. It is somewhat remarkable to observe LC behavior in LC5K-*b*-PDMS10K with the LC segment content as low as 30 wt%. All AM block copolymers from AM5K oligomer and PDMS

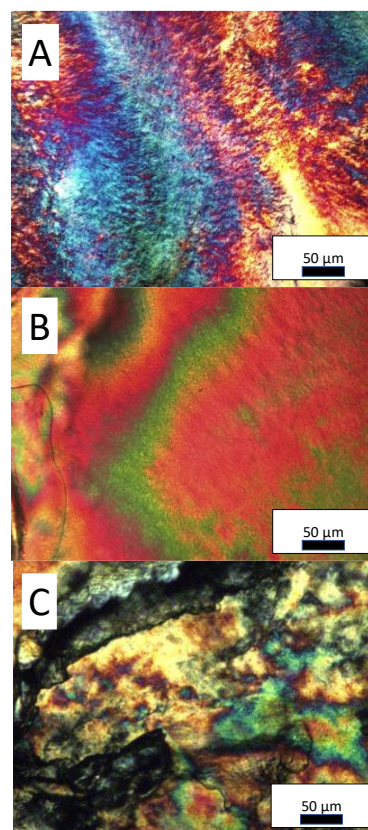


**Fig. 3.** Microphotographs of the (AB)<sub>n</sub> multiblock copolymers observed between crossed polarizers at  $300\text{ }^\circ\text{C}$  at a heating rate of  $20\text{ }^\circ\text{C}\cdot\text{min}^{-1}$ . **A-** LC5K-*b*-PDMS1K; **B-** LC5K-*b*-PDMS5K; **C-** LC5K-*b*-PDMS10K.

segments show isotropic phase behavior as a function of temperature. The microphotographs of the LC textures confirming the thermotropic nematic nature of the segmented block copolymers are shown in Figure 3.

#### Dynamic mechanical Thermal Analysis (DMTA)

AM5K-*b*-PDMS block copolymers thin films were prepared by casting a 10% w/v solution from chloroform (filtered through a  $5\text{ }\mu\text{m}$  pore size PTFE syringe filter) into a level 8 cm diameter petri dish. The solvent was allowed to evaporate at  $30\text{ }^\circ\text{C}$  in an

**Table 4.** Summary of key thermal properties as collected by TGA, DSC and DMTA.

Sample	TGA <sup>1</sup>		DSC		DMTA			
	$T_d^{5\%}$ ( $^\circ\text{C}$ )	Char yield (wt%)	$T_{g1}^2$ ( $^\circ\text{C}$ )	$T_{g2}^3$ ( $^\circ\text{C}$ )	$E'$ (GPa) <sup>4</sup> ( $25\text{ }^\circ\text{C}$ )	$E'$ (GPa) <sup>4</sup> ( $100\text{ }^\circ\text{C}$ )	$T_{g1}^5$ ( $^\circ\text{C}$ )	$T_{g2}^6$ ( $^\circ\text{C}$ )
AM5K- <i>b</i> -PDMS1K	346	37	-	120	5.2	1.4	-	96
AM5K- <i>b</i> -PDMS5K	381	28	-129	120	2.3	0.9	-127	102
AM5K- <i>b</i> -PDMS10K	427	20	-124	124	1.5	0.06	-126	103
LC5K- <i>b</i> -PDMS1K	358	40	-	-	3.5	1.8	-	112
LC5K- <i>b</i> -PDMS5K	390	27	-128	-	0.6	0.3	-127	112
LC5K- <i>b</i> -PDMS10K	423	21	-119	-	0.3	0.1	-124	115

<sup>1</sup>  $T_d^{5\%}$  represents the 5% weight loss under nitrogen at a heating rate of  $10\text{ }^\circ\text{C}\cdot\text{min}^{-1}$ , Char yield is defined as the residual weight at  $600\text{ }^\circ\text{C}$  under nitrogen atmosphere;

<sup>2</sup> Glass transition ( $T_{g1}$ ) of PDMS blocks at a heating rate of  $40\text{ }^\circ\text{C}\cdot\text{min}^{-1}$ , under a helium atmosphere;

<sup>3</sup> Glass transition ( $T_{g2}$ ) of aromatic blocks at a heating rate of  $40\text{ }^\circ\text{C}\cdot\text{min}^{-1}$ , under a helium atmosphere;

<sup>4</sup> Storage modulus ( $E'$ ) collected by DMTA at 1Hz, using a heating rate of  $2\text{ }^\circ\text{C}\cdot\text{min}^{-1}$ ;

<sup>5</sup> Glass transition ( $T_{g1}$ ) of aromatic blocks at a heating rate of  $40\text{ }^\circ\text{C}\cdot\text{min}^{-1}$ , under a helium atmosphere;

<sup>6</sup> Glass transition ( $T_{g2}$ ) of PDMS blocks at a heating rate of  $40\text{ }^\circ\text{C}\cdot\text{min}^{-1}$ , under a helium atmosphere;

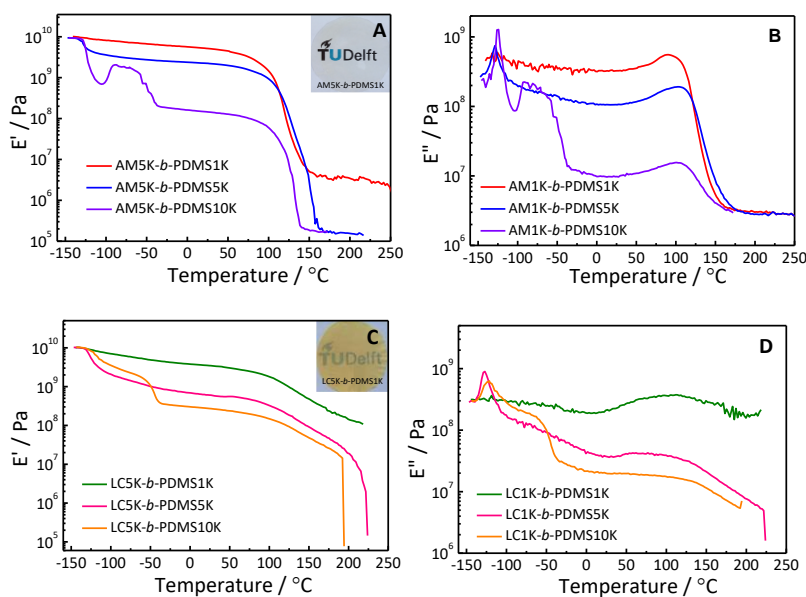


**Fig. 4.** DMTA analysis of the multiblock copolymers. **A-** and **C-** Storage modulus ( $E'$ ) as a function of temperature for the AM5K-*b*-PDMS series and LC5K-*b*-PDMS series, respectively; **B-** and **D-** loss modulus ( $E''$ ) as function of temperature for the AM5K-*b*-PDMS series and LC5K-*b*-PDMS series, respectively. All analyses were conducted using a heating rate of 2 °C·min<sup>-1</sup> under N<sub>2</sub> atmosphere and at a frequency of 1 Hz. The insets in **A** and **C** show the films from AM5K-*b*-PDMS1K and LC5K-*b*-PDMS1K, respectively.

oven overnight. When most of the solvent was removed, the transparent film was dried at 100 °C under vacuum for 2 h, to remove residual solvent. Due to the difference in solubility, thin films prepared from the LC5K-*b*-PDMS block copolymers were cast from TCE. The cast films were dried in an oven at 60 °C overnight and residual solvent was removed by drying at 150 °C under vacuum for 2h. All the freestanding films were obtained after soaking the petri dish in lukewarm water. DMTA experiments were performed on all segmented block copolymer films prepared as stated above, with the aim to investigate the storage modulus ( $E'$ ) and loss modulus ( $E''$ ) as a function of temperature, and the results are shown in Figure 4. Table 4 summarizes the DMTA results.

The AM series of the segmented block copolymers shows similar storage moduli at -150 °C, at approximately 10 GPa (Figure 4), indicating the stiff nature of the block copolymer at cryogenic temperatures. The storage moduli are hardly affected by the block copolymer compositions at temperatures below  $T_g$  of PDMS. No obvious decrease in modulus at around -125 °C was observed for AM5K-*b*-PDMS1K, indicative of the low PDMS content. The drop in  $E'$  for AM5K-*b*-PDMS5K and AM5K-*b*-PDMS10K is more significant as their PDMS blocks are larger. The  $T_g$ s of the aromatic blocks of the three AM multiblock copolymers were observed at approximately 100 °C. Between the two  $T_g$ s, a stable modulus plateau was observed, characteristic of thermoplastic elastomers (TPEs).<sup>33</sup> The AM5K-*b*-PDMS10K film exhibits cold crystallization of PDMS when the film was heated above the  $T_g$  of the PDMS segments, at -89 °C. Subsequent heating induced melting of the PDMS crystals, which was also confirmed by DSC experiments.

For the LC5K-*b*-PDMS multiblock copolymer series, similar results were obtained in the DMTA tests. Only one  $T_g$  originating

from the rigid aromatic block was observed for LC5K-*b*-PDMS1K, due to the very low content of PDMS. LC5K-*b*-PDMS5K shows two obvious  $T_g$ s, again indicative of (micro)phase separation.<sup>28, 29, 33</sup> The curve of LC5K-*b*-PDMS10K shows a drop in  $E'$  at -50 °C, which is attributed to melting of the PDMS crystals, as confirmed by our DSC results.

It is remarkable to observe that the storage moduli of the AM5K-*b*-PDMS multiblock copolymers are greater to those of the LC5K-*b*-PDMS analogs. This is likely due to the intermixing of the two blocks in the block copolymers. The degree of intermixing in phase-separated multiblock copolymers depends in part on the flexibility of the segments. Block copolymers comprised of two amorphous phases typically show a higher degree of intermixing than block copolymers based on amorphous/nematic phases.<sup>3</sup> By a larger degree of mixing, the properties of the aromatic (stiff) units are better dispersed, resulting in bulk properties resembling a mixed character of the two constituents.

#### WAXD analysis of multiblock copolymers

The morphology of the aromatic/PDMS multiblock copolymer films was analyzed by room temperature WAXD experiments and the results are shown in Figure 5.

From the one-dimensional X-ray diffraction intensity profiles of the AM multiblock copolymers in Figure 5A, the broad diffraction peak at  $2\theta = 12^\circ$  ( $d$ -spacing = 7.4 Å) is characteristic of amorphous PDMS.<sup>34</sup> The characteristic peak at  $2\theta = 20^\circ$  of amorphous polymers is attributed to the inter-chain  $d$ -spacing ( $d = 4.4$  Å).<sup>32</sup> Similar to the AM multiblock copolymer, LC multiblock copolymer films show a broad diffraction peak at  $2\theta = 12^\circ$  ( $d = 7.4$  Å) attributed to the PDMS tetragonal crystal lattice, see Figure 5B. The intense diffraction peak at  $2\theta = 18^\circ$  ( $d = 4.8$  Å) is again attributed to the interchain  $d$ -spacing, similar

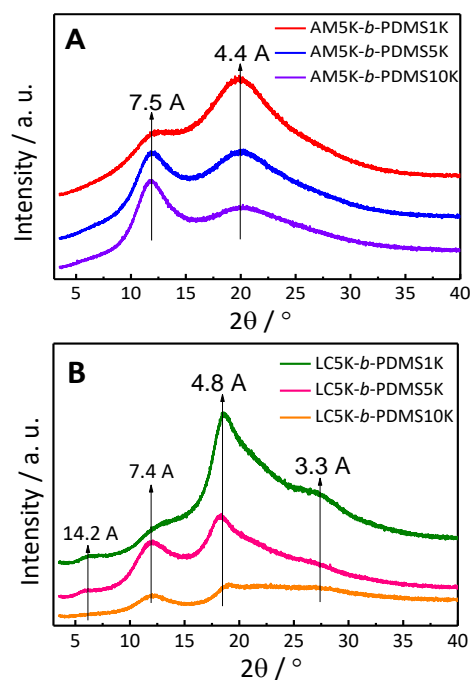


**Fig. 5.** WAXD analysis of the AM-PDMS and LC-PDMS block copolymers. 1-dimensional WAXD diffraction intensity profiles of **A-** AM multiblock copolymer films, and **B-** LC multiblock copolymer films at room temperature. The curves are offset for clarity.

to what is observed for the AM series. The diffraction peak located at  $2\theta = 6.2^\circ$  ( $d = 14.2 \text{ \AA}$ ) is associated with the projection length of one repeating unit in the crystalline unit cell. The reflection at around  $27^\circ$  is ascribed to  $d_{310}$ , as reported in literature.<sup>35</sup> The existence of distinct diffraction peaks for PDMS and the aromatic domains again confirms (micro)phase separation, as was also observed by DMTA and DSC experiments.

### Transmission Electron Microscopy and Atomic Force Microscopy analysis

As confirmed by DSC, DMTA and WAXD experiments, (micro)phase separation occurs in this type of aromatic/PDMS segmented block copolymer. Figure 6 shows the transmission electron micrographs of ultrathin sections of the AM5K-*b*-PDMS and LC5K-*b*-PDMS multiblock copolymers prepared by cryo-microtome. Due to the high electron density of PDMS compared to the aromatic polyester, no staining is needed and the black and white areas indicate a PDMS-rich and an ester-rich domain, respectively.<sup>36</sup>

In the TEM microphotographs of the AM5K-*b*-PDMS multiblock copolymers, no obvious phase separation was observed for AM5K-*b*-PDMS1K, whereas in AM5K-*b*-PDMS5K, micro-phase separation, with domains on the order of  $\sim 50 \text{ nm}$ , can be seen. Somewhat larger feature sizes ( $\sim 100 \text{ nm}$ ) can be observed in AM5K-*b*-PDMS10K. In the LC5K-*b*-PDMS series, phase separation is clearly observable for all 3 samples. Especially in LC5-*b*-PDMS5K, the LC- and PDMS-fractions are distinctly separated in dark (PDMS) and light (polyester) domains that are on the order of 50–300 nm. Pospiech and colleagues reported similar observations in that block copolymer systems based on two different amorphous phases typically show a high degree of intermixing between the phases, while in systems comprised of an amorphous phase and a nematic phase, less intermixing is observed.<sup>3</sup> AFM analysis of sample cross-sections ( $5 \mu\text{m} \times 5 \mu\text{m}$ ) yields a similar picture. The segmented AM5K block copolymers show a higher degree of intermixing whereas the LC5K block copolymers clearly show phase separated domains. The AFM phase maps and height maps are available in the SI (Figures S7 and S8).

### Thin film tensile properties

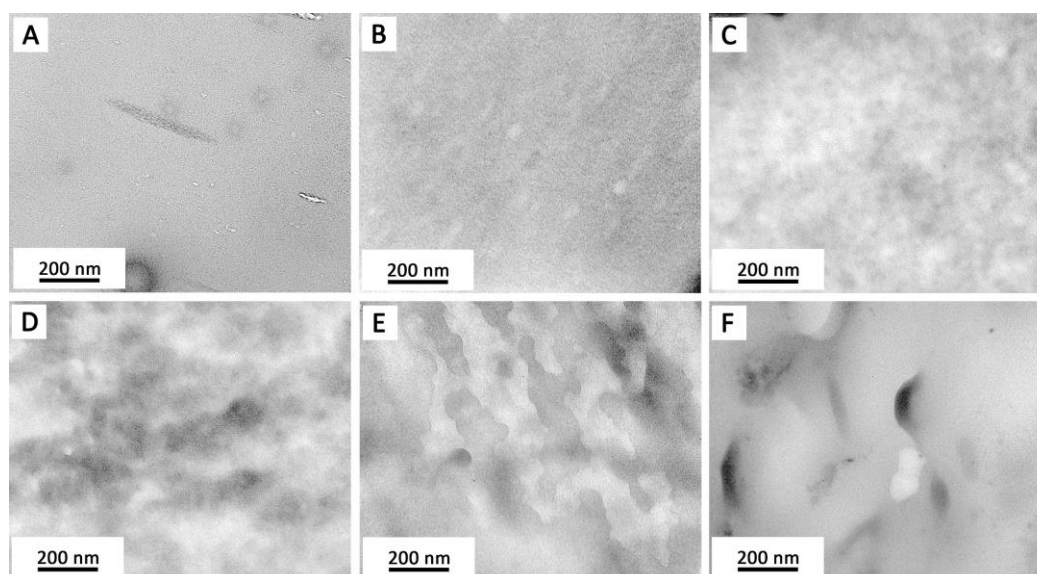


**Fig. 6.** Cryo-TEM images of the  $(AB)_n$  multiblock copolymers. **A-** AM5K-*b*-PDMS1K; **B-** AM5K-*b*-PDMS5K; **C-** AM5K-*b*-PDMS10K; **D-** LC5K-*b*-PDMS1K; **E-** LC5K-*b*-PDMS5K; **F-** LC5K-*b*-PDMS10K.



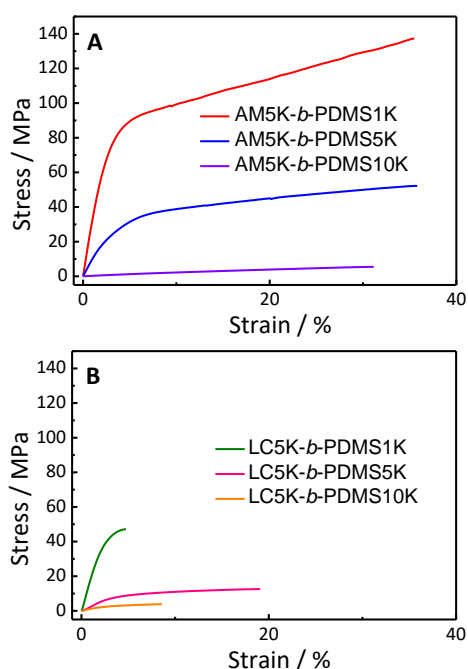


**Fig. 7.** Room temperature stress-strain results. **A-** AM5K-*b*-PDMS series and **B-** LC5K-*b*-PDMS multiblock copolymer series. Shown are the best results out of 5 stress-strain experiments. All experiments were performed at a strain rate of 0.1 mm/mm·min<sup>-1</sup>.

The tensile behavior of the thin films tested at 22 °C is shown in Figure 7 and 8, and the data is summarized in Table 5. Prior to film casting, filtration of the casting solution through a 5 μm syringe filter was performed to remove insoluble particulates and to avoid any irregularities in the resulting films. The films are flexible and easy to handle, and can be cut into test specimen without difficulty. The best tensile properties of the as-prepared films out of 5 experiments are shown in Figure 7.

Overall, the tensile properties of the thin films are dependent on the PDMS chain length (associated with PDMS contents) in the multiblock copolymers. With an increase in PDMS content, the tensile strength and elastic modulus of the multiblock copolymers decrease dramatically. Over the whole composition range, the AM5K-*b*-PDMS block copolymer films show average tensile strength and elastic moduli ranging from 5.2 to 123.6 MPa and 0.03 to 3.4 GPa, respectively. In sharp contrast, the LC5K-*b*-PDMS series shows much lower average tensile data. The LC5K-*b*-PDMS1K displays an average tensile

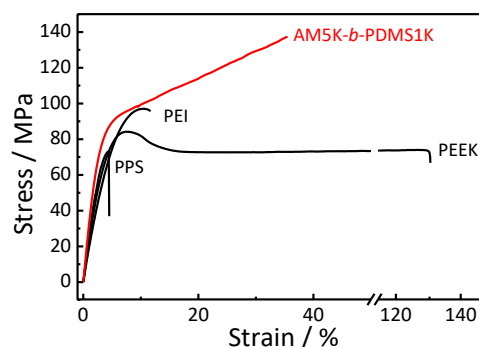


**Fig. 8.** Tensile properties of the AM5K-*b*-PDMS1K film contrasted with commercial high-performance polymer films, *i.e.*, PEEK (TenCate Cetex® TC1200), PEI (TenCate Cetex® TC1000) and PPS (TenCate Cetex® TC1100).

strength and elastic modulus of 38.4 MPa and 1.6 GPa, respectively. With the PDMS chain length increasing to 10K, the LC5K-*b*-PDMS10K shows an average tensile strength and elastic modulus of 3 MPa and 0.013 GPa, respectively. It is also clear that the hard segments have a great effect on the tensile properties of the block copolymer films. In general, the AM5K-*b*-PDMS-based multiblock copolymers show increased mechanical properties, *i.e.* elastic moduli, tensile strength, fracture strain and toughness over their LC5K-based analogs. Take AM5K-*b*-PDMS1K and LC5K-*b*-PDMS1K as examples, the tensile strength is 123.6 and 38.4 MPa, respectively, and the elastic moduli are 3.4 and 1.6 GPa, respectively. The AM5K-*b*-PDMS1K film exhibits a much higher fracture elongation (31%) and toughness (30.7 MJ·m<sup>-3</sup>) when compared to LC5K-*b*-PDMS1K (3.5% and 1 MJ·m<sup>-3</sup>, respectively). This is because the LC5K-based multiblock copolymers have a higher degree of microphase separation, as confirmed by TEM results (Figure 6). Typically, a non-phase separated multiblock copolymer show higher modulus than their phase separated analogs.<sup>37, 38</sup> The higher mechanical properties of AM5K-*b*-PDMS1K is the result of a higher degree of phase intermixing (Figure 6). Similar behavior was reported for other multiblock copolymers, such as polysulfone-*b*-PDMS, polyamide-*b*-PDMS, polyether-*b*-polyamide, polybutadiene-*b*-polyamide.<sup>18, 19, 39-42</sup>

Since the mechanical performance of polymer materials are highly dependent on the testing conditions, a comparison of the tensile behavior with some commercial high-performance

**Table 5.** Average tensile properties of 5 film specimens of the (AB)<sub>n</sub> block copolymers and commercial polymers.

Samples	Tensile strength (MPa)	Elastic modulus (GPa)	Elongation at break (%)	Toughness (MJ·m <sup>-3</sup> )
AM5K- <i>b</i> -PDMS1K	123.6±15.4	3.4±0.2	31.2±4.0	30.7±5.8
AM5K- <i>b</i> -PDMS5K	48.7±2.4	1.1±0.06	26.1±5.5	10.7±2.3
AM5K- <i>b</i> -PDMS10K	5.2±0.3	0.03±0.002	27.5±2.9	0.8±0.1
LC5K- <i>b</i> -PDMS1K	38.4±6.0	1.6±0.2	3.5±0.9	1.0±0.3
LC5K- <i>b</i> -PDMS5K	11.6±0.7	0.3±0.07	16.9±2.2	1.9±0.8
LC5K- <i>b</i> -PDMS10K	3.0±0.2	0.01±0.001	8.6±1.5	0.2±0.1
PEEK	78.9±4.6	2.3±0.1	123.7±13.7	84.9±10
PEI	93.2±8.0	2.1±0.1	10.7±1.8	7.7±1.4
PPS	72.3±1.8	2.5±0.1	4.2±0.4	1.9±0.2

polymer films was made under the same test conditions. Figure 8 shows the best performing data out of 5 tensile experiments of PEEK (TenCate Cetex<sup>®</sup> TC1200), PEI (TenCate Cetex<sup>®</sup> TC1000) and PPS (TenCate Cetex<sup>®</sup> TC1100) films, as well as AM5K-*b*-PDMS1K. It is clear that the AM5K-*b*-PDMS1K film shows the highest tensile strength (123.6 MPa) and elastic modulus (3.4 GPa), with a high elongation at break (31%) and toughness (30.7 MJ·m<sup>-3</sup>), while the PEEK film shows the highest fracture elongation (123.7%) and toughness (84.9 MJ·m<sup>-3</sup>) due to necking.

#### Thin film shape memory performance

Block copolymers are promising shape memory materials, because of their nanophase separated morphology,<sup>43</sup> where the individual domains can act as switches for the different shape changes, as shown in Figure 9. When combining polymer blocks that have a high aromatic content with soft PDMS blocks it should be possible to design block copolymers that exhibit both excellent strength and a shape-memory function over a very broad (~200 °C) temperature range. In a study by Thorsten and coworkers, a triple SM multiblock poly(ester urethane) was reported.<sup>44</sup> This polymer displays a triple-shape functionality in the temperature range of -60 to 60 °C, using the crystallization temperature ( $T_c$ ) of the soft segment and the glass transition temperature ( $T_g$ ) of the rigid segment as the triggers. Polyethyleneoxide was utilized in segmented multiblock copolymers with poly(ethylene terephthalate) (PET) hard blocks.<sup>45</sup> Polyamides and aramids were also used as hard blocks in combination with poly( $\epsilon$ -caprolactone) to prepare multiblock copolymers with shape memory characteristics.<sup>46, 47</sup> However, to the best of our knowledge, none of the reported materials show a shape-memory effect (SME) at both high temperature (> 150 °C) and at low temperature (< -150 °C) at the same time. Another shortcoming is that all these polymers have rather low moduli, due to the high concentrations of soft segments, which

limits their application as shape-memory materials to soft, non-structural applications only.

Traditionally, a quantitative characterization of the SME is conducted using a cyclic thermo-mechanical extension or bending test.<sup>48</sup> However, the multiblock copolymers are not chemically crosslinked, and elastic deformations are only observed in a region with strain less than 5% in stress-strain curves. As a result, an orientation of the multiblock copolymer films could take place during SM testing if a cyclic thermo-mechanical extension is applied, making SME characterization not possible. SME characterization using a torsion mode set-up was also reported by Diani *et al.*<sup>49</sup> Torsion mode testing involves non-homogeneous strains and stresses in the cross-section of a rectangular film sample, and enables the SMPs to reach large deformations with moderate strains.<sup>50</sup> Thus, a torsion mode setup was used to characterize the SME of our multiblock copolymer films. The deformation and fixation of the film samples are performed under strain control, and the recovery is in a stress-free condition.

#### Dual Shape memory properties of AM5K-/LC5K-*b*-PDMS1K block copolymer films

As discussed above, the AM5K-*b*-PDMS1K multiblock copolymer shows one  $T_g$  only, covering the temperature range from 100–150 °C (Figure 4A). Two stable plateaus with  $E'$  of approximately 5 GPa and 4 MPa, respectively, can be observed before and after  $T_g$ . The presence of two plateau regions (<  $T_g$  and >  $T_g$ ) is of interest, as this facilitates high-temperature shape memory behaviour.<sup>51</sup> Besides, this material shows excellent tensile strength (> 123 MPa) and elastic modulus (> 3.4 GPa) in tensile testing experiments at 22 °C, making this material a promising engineering SMP. In the case of LC5K-*b*-PDMS1K, again only one  $T_g$  was observed (Figure 4C) from DMTA, but the glass transition temperature range is wider. Both AM5K-*b*-PDMS1K and LC5K-*b*-PDMS1K were investigated using the torsion mode method.

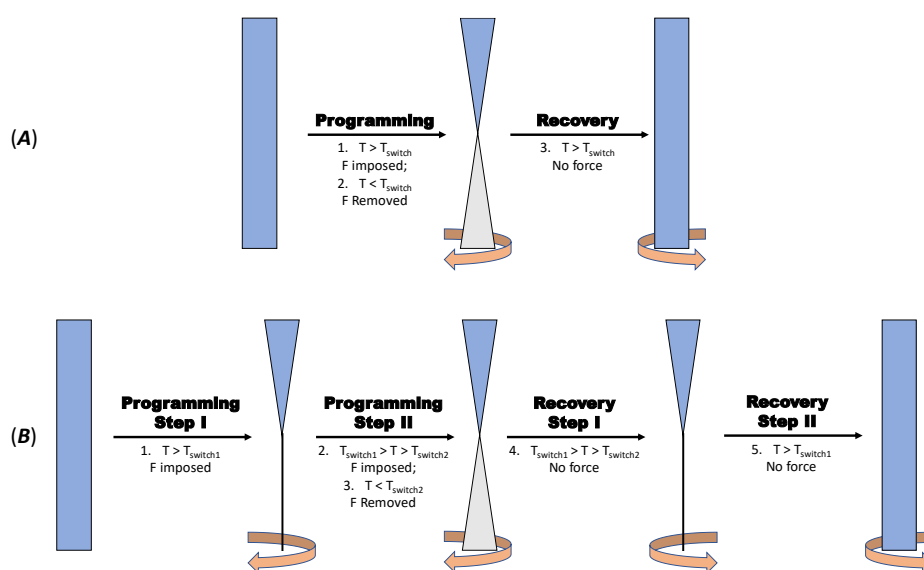


**Fig. 9.** Schematic representation of the torsion mode shape memory tests used. **A-** dual-SME; **B-** triple-SME.  $T_{switch}$  is the switching temperature of the SMPs.

Three consecutive deformation, fixation and recovery cycles were performed for each sample to test the shape memory behaviour over multiple cycles. The results are shown in Figure S9, and the  $R_f$  and  $R_r$  are calculated using Equation 5 and 6 (see Characterization under Experimental section), and summarized in Table 6.

During the dual-SM test, the multiblock copolymer film samples were deformed at 150 °C, which is well above  $T_g$  (96 °C and 112 °C for AM5K-*b*-PDMS1K and LC5K-*b*-PDMS1K, respectively, and the temporary shape was fixed at 20 °C. At this temperature, the mobility of the polymer chain segments is strongly restricted by the rigid domains. However, this is not sufficient to fix the deformation (torsion) and with the release of the imposed force, the sample relaxed, resulting a slight reduction in torsional angle. This was also observed in other physical scaffolds systems.<sup>52</sup> With the temperature increase to 150 °C, the temporary shape recovers to its original permanent shape, triggered by the glass transition of the rigid segments. The dual shape fixation and recovery results of the two materials are summarized in Table 6.

The AM5K-*b*-PDMS1K film shows a high  $R_f$  value of approximately 100% in the three cycles, whereas the  $R_r$  numbers of LC5K-*b*-PDMS1K film are slightly lower (97% in the three cycles). The AM5K-*b*-PDMS1K film shows a high  $R_r$  of approximately 97% - 98% over the three cycles, while the LC5K-*b*-PDMS1K film shows a recovery with a medium  $R_r$  value of 88% in the first cycle, and 81% in the third cycle. Most likely, this is because LC5K-*b*-PDMS1K is semi-crystalline and AM5K-*b*-PDMS1K is totally amorphous. The shape recovery originates from the relaxation of the amorphous chain segments, which are restricted by the crystalline domains. The recovery of all samples cannot reach 100% because of the inevitable irreversible chain-segment orientation and relaxation effects, which partly dissipate the stored stresses.<sup>53</sup> The shape recovery velocity as a function of temperature results are summarized in Table 6 (Figure S9). Both samples show relatively low velocity (< 25 °·min<sup>-1</sup>) at 143 °C through the recovery process, which is a general phenomenon among  $T_g$ -based SMPs.<sup>54</sup> The shape recovery is triggered by the glass transition of the amorphous

chain segments, which is significantly slower than other transitions, such as melting.

#### Triple Shape memory properties of AM5K-/LC5K-*b*-PDMS5K block copolymer films

In contrast to AM5K-*b*-PDMS1K and LC5K-*b*-PDMS1K, the PDMS5K-based analogous films exhibit three stable storage moduli ( $E'$ ) plateau regions ( $> T_{g1}$ ,  $T_{g2} - T_{g1}$  and  $< T_{g2}$ ) (Figure 4). The  $T_g$  is very low for the PDMS segments (-125 °C) and high for the rigid units (102 and 112 °C for AM5K and LC5K, respectively). The all-aromatic microphases act as physical net-points, together with the appearance of the two distinct glass transitions, making the two polymers potential triple SMPs. The two  $T_g$ s of the two (micro)phases are used as the switching temperatures to explore the triple SME.

The experimental results of the AM5K-*b*-PDMS series are shown in Figure S10, and the shape memory properties of the multiblock copolymers are summarized in Table 6. In a typical experiment, after cooling to -150 °C, the shape fixation rate  $R_f$  of the multiblock copolymer films are 96 and 88% for AM5K-*b*-PDMS5K and LC5K-*b*-PDMS5K, respectively. While heating up to recovering temperature, both of the AM5K-*b*-PDMS5K and LC5K-*b*-PDMS5K show  $R_{r(C\rightarrow B)}$  and  $R_{r(B\rightarrow A)}$  values of 96 % and 99% for AM5K-*b*-PDMS5K, while those for LC5K-*b*-PDMS5K are 80% and 91%, respectively. As listed in Table 6, the shape fixation and recovery rate remain comparable to the duplicate experiments, indicating good reproducibility.

The recovery velocity of the AM5K-*b*-PDMS5K and LC5K-*b*-PDMS5K (Figure S10) and the  $T_r$ s are summarized in Table 6, to show the validity of using the glass transitions as triggers for SME. The AM5K-*b*-PDMS5K multiblock copolymer film was heated from the temporary shape *C* at -150 °C showing an obvious recovery velocity peak located at -131 °C, due to the  $T_g$  of the PDMS blocks. Further heating to ~50 °C, the film is further recovering from shape *C* to *B* slowly, indicating a slow relaxation of the hindered PDMS block among the AM5K blocks. A much higher recovery velocity peak at 139 °C due the  $T_g$  of the AM5K blocks is observed releasing all the stress from the system and restoring the original shape. Similar to AM5K-*b*-PDMS5K, LC5K-

**Table 6.** Dual- and triple- shape fixation and recovery results of the (AB)<sub>n</sub> multiblock copolymer films.

Samples	$T_g^1$ (°C)	$T_{prog}^2$ (°C)	$T_r^3$ (°C)	Cycle 1		Cycle 2		Cycle 3	
				$R_f$ (%) <sup>4</sup>	$R_r$ (%) <sup>5</sup>	$R_f$ (%) <sup>4</sup>	$R_r$ (%) <sup>5</sup>	$R_f$ (%) <sup>4</sup>	$R_r$ (%) <sup>5</sup>
AM5K- <i>b</i> -PDMS1K	96	150	143	100	98	100	97	100	97
LC5K- <i>b</i> -PDMS1K	112	150	143	97	88	97	85	97	81
AM5K- <i>b</i> -PDMS5K	-127, 102	150, 20	-131, 139	96	96 (C→B), 99 (B→A)	95	99 (C→B), 99 (B→A)	95	99 (C→B), 99 (B→A)
LC5K- <i>b</i> -PDMS5K	-127, 112	150, 20	-129, 136	93	88 (C→B), 80 (B→A)	91	87 (C→B), 89 (B→A)	92	85(C→B), 83 (B→A)

<sup>1</sup> Glass transition temperature ( $T_g$ ) reported as the maximum of the loss modulus ( $E''$ ) at 1 Hz in DMTA experiments (from Figure 4). <sup>2</sup>  $T_{prog}$  is the programming temperature. <sup>3</sup>  $T_r$  is the temperature at maximum recovery velocity. <sup>4</sup>  $R_f$  is the fixation rate. <sup>5</sup>  $R_r$  (C→B) refers the recovery rate from shape C to shape B;  $R_r$  (B→A) refers the recovery rate from shape B to shape A.

*b*-PDMS5K exhibits slow recovery below 50 °C starting at the  $T_g$  of the PDMS phase, together with a high recovery velocity at ~130 °C. The experiment clearly shows the SME of this type of multiblock copolymers is triggered by the glass transition temperatures. With a similar trend as the PDMS1K based multiblock copolymers, the AM5K-*b*-PDMS5K films shows increased fixation rate and recovery rate over its LC5K-based analogs for similar reasons as discussed above.

Noteworthy, even though the multiblock copolymers with PDMS10K also show two  $T_g$ s (DMTA results, Figure 4 and Table 4), no triple or dual high temperature SME was observed. This is most likely due to the very low concentration of physical crosslinkers, *i.e.* the aromatic part of the polymer backbone, which is not sufficient to provide a scaffold that locks the temporary shapes.<sup>55</sup>

## Experimental

### Materials

All chemicals were obtained from the indicated sources and used as received unless stated otherwise. 1,1,2,2-tetrachloroethane (TCE, 98%) were purchased from Acros Organics. Prior to use, TCE was dried over CaH<sub>2</sub> at 120 °C for 5 h and distilled under vacuum at 125 °C. Triethylamine (NEt<sub>3</sub>, 99%), from Sigma-Aldrich, was dried over CaH<sub>2</sub> at 100 °C for 5 h and distilled prior to use. Hexane (99%) was purchased from VWR and refluxed over CaH<sub>2</sub> under nitrogen atmosphere to remove moisture. Hexane was dried and stored over CaH<sub>2</sub> and distilled when needed. Phenyl hydroquinone (PHQ, 97%) was obtained from Sigma Aldrich and recrystallized twice from chloroform under N<sub>2</sub> atmosphere. After recrystallization, PHQ was dried under vacuum at 60 °C for 24 h. Telechelic hydroxyl-functionalized poly(dimethyl siloxane)s with various number average molecular weights ( $M_n$ ), of 1.0, 5.0 and 10 kg·mol<sup>-1</sup> were purchased from Gelest Inc. The PDMS oligomers were labelled as PDMS1K-OH, PDMS5K-OH and PDMS10K-OH, respectively, where PDMS-OH reflects the main-chain and end-groups and the integers refer to the molecular weight, *i.e.* 1K = 1.0 kg·mol<sup>-1</sup>. The following chemicals were purchased from Sigma-Aldrich and used without further purification: maleic anhydride (99%), *p*-aminophenol (99%), sulfuric acid (98%), *N,N*-dimethylformamide (DMF, 99.8%), phosphorus pentoxide (P<sub>2</sub>O<sub>5</sub>, 99%), 2-bromo-1,4-dimethylbenzene (99%), Tetrakis(triphenylphosphine) palladium(0) (Pd(PPh<sub>3</sub>)<sub>4</sub>, 99%), Na<sub>2</sub>CO<sub>3</sub> (99%), phenylboronic acid (95%), H<sub>2</sub>O<sub>2</sub> (30%), pyridine (99%), potassium permanganate (99%), thionyl chloride (99%), and hydrochloric acid (30%), anhydrous toluene (99.8%), anhydrous tetrahydrofuran (THF, 99.9%), mesyl chloride (99.7%), magnesium sulfate (MgSO<sub>4</sub>, 98%), Celite 545, hydrochloric acid (30%) and *n*-propylamine (98%). Potassium thioacetate (98%) was purchased from Acros Organics. Ethanol, dichloromethane (DCM), sodium chloride, diethyl ether and toluene were purchased from VWR. Deuterated solvents dimethyl sulfoxide (DMSO-*d*<sub>6</sub>, 99.9% D), CDCl<sub>3</sub> (99.8% D), deuterated trifluoroacetic acid (TFA-*d*, 99.5% D), and deuterated tetrachloroethane (TCE-*d*<sub>2</sub>, 99.5% D) were all

purchased from Sigma Aldrich and used as received for NMR measurements.

### Synthesis of *N*-(4-hydroxyphenyl) maleimide

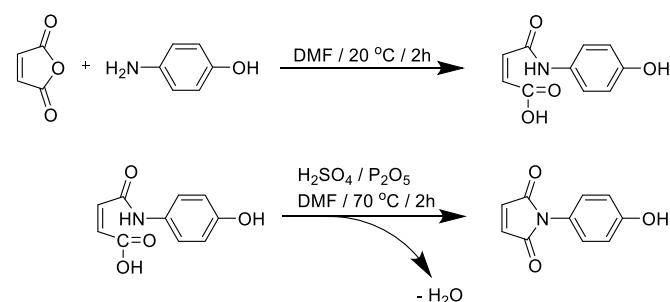
The synthesis of *N*-(4-hydroxyphenyl) maleimide (HPM) was based on literature procedures<sup>22-25</sup> and is depicted in scheme 2.

A 250 mL round-bottom flask with magnetic stirring was charged with 16.37 g (0.15 mol) of *p*-aminophenol and 50 mL of DMF. A solution of 14.71 g (0.15 mol) maleic anhydride in 50 mL DMF was added dropwise. The solution was stirred at room temperature for 2 h, followed by the addition of 12.00 g P<sub>2</sub>O<sub>5</sub> in 10 mL H<sub>2</sub>SO<sub>4</sub> and 70 mL DMF. The mixture was allowed to stir for additional 2 h at 70 °C to complete the reaction. The reaction mixture was then cooled in an ice bath and subsequently poured into 1 L cold water. The yellow precipitate was filtered, washed with water and recrystallized twice from isopropanol. This reaction yielded yellow needle-like crystals, which were dried under vacuum at 60 °C overnight. Yield: 20.20 g (71%). *m.p.*: 182 °C (lit: 182 - 184 °C<sup>22</sup>); <sup>1</sup>H NMR (DMSO-*d*<sub>6</sub>, 400 MHz)  $\delta$ : 9.69 (s, OH); 7.13 (s, 2H); 7.07 (d, *J* = 8.7 Hz, 2H); 6.84 (d, *J* = 8.7 Hz, 2H). <sup>13</sup>C NMR (DMSO-*d*<sub>6</sub>, 100 MHz)  $\delta$ : 170.74, 157.45, 134.94, 128.84, 122.94, 115.85 ppm. MS *m/z* (relative intensity): 189.00 (100%, M+), 52.10 (73), 119.05 (65), 54.10 (64), 53.10 (35), 79.10 (24), 107.10 (24), 133.10 (23), 51.15 (22), 120.10 (21).

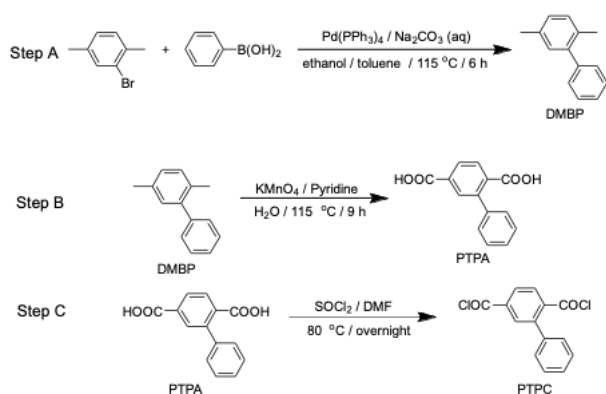
### Synthesis of phenylterephthaloyl chloride

Phenylterephthaloyl chloride (PTPC) was synthesized according to a modified literature procedure, as shown in scheme 3.

**Synthesis of 2,5-dimethyl-biphenyl (DMBP):** A 2-L three-necked flask equipped with an overhead mechanical stirrer and reflux condenser was charged with 46.27 g (250 mmol) of 2-bromo-1,4-dimethylbenzene, 500 mL of toluene and 250 mL of an aqueous solution of 2 mol·L<sup>-1</sup> Na<sub>2</sub>CO<sub>3</sub> under an argon atmosphere. A solution of 32.00 g (262.50 mmol) of phenylboronic acid in 125 mL of ethanol was added, followed by 1.5 g (1.3 mmol) of Pd(PPh<sub>3</sub>)<sub>4</sub> as catalyst. After degassing and backfilling with argon (3 times), the yellow, dual-phase mixture was refluxed at 115 °C under vigorous stirring. The reaction was monitored using TLC with hexane as the mobile phase. After the reaction was completed (6 h), the residual phenylboronic acid was oxidized by 20 mL H<sub>2</sub>O<sub>2</sub> (30%) at room temperature for 1 h. The reaction mixture was extracted with ether, washed with brine, and subjected to a short silica gel filtration step with hexane as eluent to remove traces of catalyst. The product



**Scheme 2.** Synthetic route towards *N*-(4-hydroxyphenyl) maleimide (HPM).



**Scheme 3.** Synthetic route towards phenylterephthaloyl chloride (PTPC).

(DMBP) was obtained as a colorless oil, which was dried under vacuum at room temperature overnight. Crude yield: 45.40 g (249.1 mmol), 99.6 %. <sup>1</sup>H NMR (DMSO-*d*<sub>6</sub>, 400 MHz): δ 2.17 (s, 3H), 2.29 (s, 3H), 7.00 (s, 1H), 7.08 (d, *J* = 7.7 Hz, 1H), 7.16 (d, *J* = 7.7 Hz, 1H), 7.27 – 7.47 (m, 5H). <sup>13</sup>C NMR (DMSO, 100 MHz): δ 141.85, 141.55, 135.18, 131.85, 130.64, 130.54, 129.30, 128.57, 128.28, 127.20, 20.94, 20.10. GC-MS *m/z* (relative intensity): *tr* = 9.1 min. 182 (100%, M<sup>+</sup>), 165 (58), 181 (36), 166 (33), 152 (28), 89 (22), 77 (16).

**Synthesis of phenylterephthalic acid (PTPA):** In a 2-L three-necked flask equipped with overhead mechanical stirrer and reflux condenser, 45.40 g (249 mmol) of DMBP was dissolved in a mixture of 750 mL of pyridine and 75 mL of H<sub>2</sub>O. After an addition of 92 g KMnO<sub>4</sub>, the mixture was allowed to reflux at 115 °C for 1 h. Over the next 8 hours, a total of 220 g of KMnO<sub>4</sub> in 500 mL of water was added in 8 portions, to the refluxing mixture. After cooling to room temperature, the phase separated mixture was filtered and the solid residual manganese dioxide was extracted twice with boiling water. The majority of pyridine from the water layer was removed by distillation under vacuum, after which dilute hydrochloric acid (10%) was added until the water layer was acidic. The precipitated white powder was filtered and washed several times with distilled water until the filtrate was neutral. After drying under vacuum at 80 °C, the crude product was recrystallized twice from glacial acetic acid. A white solid was obtained. Yield: 48.87 g (81 %). *m. p.*: 280 °C (lit: 278–280 °C<sup>26</sup>). <sup>1</sup>H NMR (DMSO-*d*<sub>6</sub>, 400 MHz): δ 7.29 – 7.49 (m, 5H), 7.81 (d, *J* = 8.0 Hz, 1H), 7.88 (s, *J* = 8.0 Hz, 1H), 7.99 (d, 1H), 13.19 (s, COOH); <sup>13</sup>C NMR (DMSO-*d*<sub>6</sub>, 100 MHz): δ 169.62, 166.94, 141.22, 140.35, 136.73, 133.05, 131.42, 129.69, 128.75, 128.65, 128.46, 128.03; MS *m/z* (relative intensity): 242 (100%, M<sup>+</sup>), 152 (87), 225 (72), 241 (50), 151 (43), 153 (39), 115 (32), 51 (31), 76 (30).

**Synthesis of phenylterephthaloyl chloride (PTPC):** A 100-mL round-bottom flask, equipped with a reflux condenser, 6.00 g (0.0248 mol) of PTPA, 30 mL of thionyl chloride and 2 drops of DMF catalyst was added under a nitrogen atmosphere and refluxed at 80 °C overnight. The slightly yellow reaction solution was cooled to 60 °C and the residual thionyl chloride was distilled off under vacuum. The remaining crude yellowish

product was recrystallized from freshly distilled dry hexane, resulting in white flakes. Yield: 6.47 g (94%). *m. p.*: 58 °C (lit: 54–55 °C<sup>26</sup>); <sup>1</sup>H NMR (DMSO-*d*<sub>6</sub>, 400 MHz): δ 7.31 – 7.51 (m, 5H), 7.82 (d, *J* = 7.8 Hz, 1H), 7.88 (s, 1H), 7.98 (d, *J* = 7.8 Hz, 1H); MS *m/z* (relative intensity): 243 (100%, [M-Cl]<sup>+</sup>), 152(73), 76 (39), 151 (37), 245 (35), 180 (21).

#### Synthesis of telechelic LC/AM5K oligomers

**AM5K:** In a 500 mL three-necked round bottom flask equipped with overhead mechanical stirrer, 9.77 g (35.00 mmol) of PTPC, 6.02 g (32.35 mmol) of PHQ and 1.00 g (5.30 mmol) of HPM were charged together with 100 mL freshly distilled, dry TCE at room temperature. After degassing and backfilling with argon, 10 mL (70 mmol) of dry triethylamine was added dropwise, while the temperature was gradually increased to 90 °C over 7 h. The turbid mixture was allowed to react at 90 °C for another 4.5 h. After the reaction was completed, the mixture was cooled to room temperature and precipitated in 500 mL of ethanol. The product was washed with hot DCM and ethanol (3 times). A white solid was obtained after drying under vacuum at 60 °C overnight. Yield: 15.01 g, 97%. <sup>1</sup>H NMR (TFA-*d*, 400 MHz): δ 8.01 – 8.38 (m), 6.81 – 7.77 (m).

**LC5K:** Following the procedure mentioned above for the synthesis of AM5K: 9.77 g (35.00 mmol) of PTPC, 3.62 g (32.83 mmol) of HQ and 0.82 g (4.33 mmol) of HPM were added to 100 mL of freshly distilled, dry TCE with the addition of 10 mL (70 mmol) of dry triethylamine as an acid scavenger. A white solid was obtained after work up. Yield: 12.67 g, 98%. <sup>1</sup>H NMR (TFA-*d*, 400 MHz): δ 8.10 – 8.40 (m), 6.84 – 7.52 (m).

#### Synthesis of thiol-terminated telechelic PDMS

The synthesis of telechelic thiol-functionalized PDMS from hydroxyl-terminated PDMS, as shown in Scheme 4, has been reported by van de Berg *et al.*<sup>30</sup> Generally, the preparation of telechelic thiol-terminated PDMS with molecular weights of approximately 1.0, 5.0 and 10 kg·mol<sup>-1</sup> were performed using the same procedure, however different molar ratios of reactants according to the various end-groups contents in PDMS were used. The synthesized samples were labelled as PDMS1K-SH, PDMS5K-SH and PDMS10K-SH, respectively, where PDMS-SH reflects the oligomer main-chain and end-groups and the integers refer to the molecular weight, *i.e.* 1K = 1.0 kg·mol<sup>-1</sup>.

**Synthesis of telechelic methylsulfonyl-terminated PDMS (PDMS-OMs):** *Telechelic PDMS1K-OMs:* Into a 100 mL three-necked flask, 27.76 g (20.00 mmol) PDMS1K-OH and 30 mL dry toluene was charged and the resulting solution was stirred under a nitrogen atmosphere. Azeotropic distillation was carried out on this clear solution at 90 °C with vigorous stirring under a steady nitrogen flow to remove traces of water. Then 60 mL anhydrous THF was added and the solution was kept under argon and cooled to 0 °C. 4.86 g (48.00 mmol) dry NEt<sub>3</sub> was added followed by a dropwise addition of 5.50 g (48.00 mmol) mesyl chloride during 10 min under vigorous stirring. Stirring was continued for 1 h at 0 °C and another 4 h at room temperature. The white precipitate was filtered off and the filtrate was diluted with diethyl ether (200 mL), washed with brine (3 × 200 mL), dried over anhydrous MgSO<sub>4</sub> and finally filtered over a short celite 545 patch. After removal of the solvent by vacuum distillation and drying under vacuum at room temperature, a clear colorless viscous liquid was obtained.



Yield: 29.24 g, 95%.  $^1\text{H NMR}$  (400 MHz,  $\text{CDCl}_3$ , ppm): 4.35 (t,  $\text{CH}_2\text{OMs}$ ), 3.68 (t,  $\text{OCH}_2\text{CH}_2\text{OMs}$ ), 3.43 (t,  $\text{CH}_2\text{OCH}_2\text{CH}_2\text{OMs}$ ), 3.04 (s,  $\text{SO}_2\text{CH}_3$ ), 1.56 – 1.63 (m,  $\text{OCH}_2\text{CH}_2\text{CH}_2$ ), 0.49 – 0.53 (broad t,  $\text{CH}_2\text{Si}$ ), -0.08 – 0.20 (m,  $(\text{CH}_3)_2\text{Si}$ ).

**Telechelic PDMS5K-OMs:** The same procedure as for telechelic PDMS1K-OMs was used, except that 23.60 g (5.00 mmol) PDMS5K-OH was treated with 1.38 g (12.00 mmol) mesyl chloride and 1.21 g (12.00 mmol)  $\text{NEt}_3$ . A clear colorless viscous liquid was obtained after work-up. Yield: 24.37 g, 100%.  $^1\text{H NMR}$  (400 MHz,  $\text{CDCl}_3$ , ppm): 4.37 (t,  $\text{CH}_2\text{OMs}$ ), 3.69 (t,  $\text{OCH}_2\text{CH}_2\text{OMs}$ ), 3.45 (t,  $\text{CH}_2\text{OCH}_2\text{CH}_2\text{OMs}$ ), 3.05 (s,  $\text{SO}_2\text{CH}_3$ ), 1.56 – 1.63 (m,  $\text{OCH}_2\text{CH}_2\text{CH}_2$ ), 0.49 – 0.53 (broad t,  $\text{CH}_2\text{Si}$ ), -0.08 – 0.22 (m,  $(\text{CH}_3)_2\text{Si}$ ).

**Telechelic PDMS10K-OMs:** The same procedure as for telechelic PDMS1K-OMs was used, except that 31.20 g (3.60 mmol) PDMS10K-OH was treated with 0.99 g (8.64 mmol) mesyl chloride and 0.87 g (8.64 mmol)  $\text{NEt}_3$ . A clear colorless viscous liquid was obtained after work-up. Yield: 30.51 g, 97%.  $^1\text{H NMR}$  (400 MHz,  $\text{CDCl}_3$ , ppm): 4.36 (t,  $\text{CH}_2\text{OMs}$ ), 3.70 (t,  $\text{OCH}_2\text{CH}_2\text{OMs}$ ), 3.45 (t,  $\text{CH}_2\text{OCH}_2\text{CH}_2\text{OMs}$ ), 3.05 (s,  $\text{SO}_2\text{CH}_3$ ), 1.56 – 1.63 (m,  $\text{OCH}_2\text{CH}_2\text{CH}_2$ ), 0.49 – 0.53 (broad t,  $\text{CH}_2\text{Si}$ ), -0.08 – 0.22 (m,  $(\text{CH}_3)_2\text{Si}$ ).

**Synthesis of telechelic thioacetyl-terminated PDMS (PDMS-TA):** **Telechelic PDMS1K-TA:** To a solution of 29.24 g (18.94 mmol) telechelic PDMS1K-OMs oligomer in 140 mL DMF, 8.65 g (75.75 mmol) potassium thioacetate was added all at once under a nitrogen atmosphere. The light red mixture was allowed to stir at 80 °C overnight. After cooling to room temperature, 200 mL water was added, which dissolved the precipitated salt to form a two-phase system. Subsequently, the mixture was extracted with diethyl ether ( $3 \times 100$  mL) and the combined organic layers were washed with brine ( $3 \times 200$  mL), dried with anhydrous  $\text{MgSO}_4$  and filtered over a short celite 545 patch. After concentrating in vacuo, a clear slightly yellow viscous liquid was obtained, which was dried under vacuum at room temperature overnight. Yield: 28.10 g, 98%.  $^1\text{H NMR}$  (400 MHz,  $\text{CDCl}_3$ , ppm): 3.53 (t,  $\text{OCH}_2\text{CH}_2\text{SAC}$ ), 3.39 (t,  $\text{CH}_2\text{SAC}$ ), 3.07 (t,  $\text{CH}_2\text{OCH}_2\text{CH}_2\text{SAC}$ ), 2.32 (s,  $\text{SCOCH}_3$ ), 1.54–1.62 (m,  $\text{OCH}_2\text{CH}_2\text{CH}_2$ ), 0.49 – 0.53 (broad t,  $\text{CH}_2\text{Si}$ ), -0.08 – 0.22 (m,  $(\text{CH}_3)_2\text{Si}$ ).

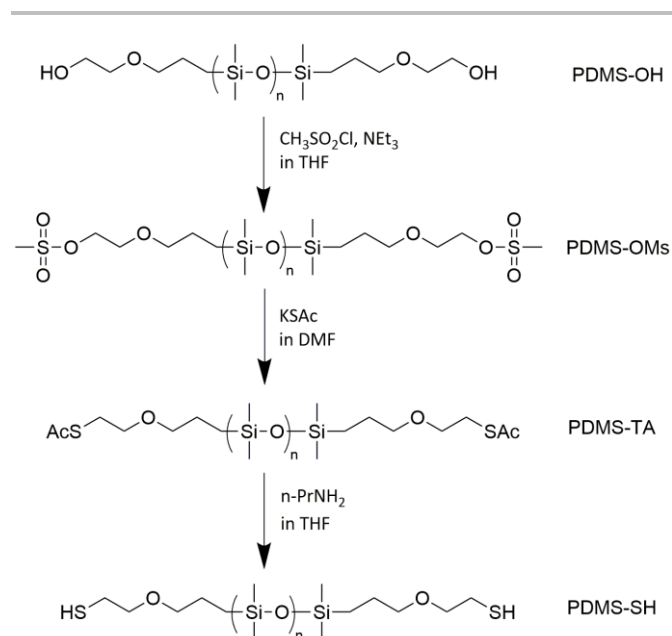
**Telechelic PDMS5K-TA:** The same procedure as for telechelic PDMS1K-TA was used, except that 24.37 g (5.00 mmol) PDMS5K-OMs was treated with 2.28 g (20.00 mmol) potassium thioacetate. A clear slightly yellow viscous liquid was obtained after work-up. Yield: 23.68 g, 98%.  $^1\text{H NMR}$  (400 MHz,  $\text{CDCl}_3$ , ppm): 3.54 (t,  $\text{OCH}_2\text{CH}_2\text{SAC}$ ), 3.40 (t,  $\text{CH}_2\text{SAC}$ ), 3.08 (t,  $\text{CH}_2\text{OCH}_2\text{CH}_2\text{SAC}$ ), 2.33 (s,  $\text{SCOCH}_3$ ), 1.54–1.62 (m,  $\text{OCH}_2\text{CH}_2\text{CH}_2$ ), 0.49 – 0.53 (broad t,  $\text{CH}_2\text{Si}$ ), -0.08 – 0.22 (m,  $(\text{CH}_3)_2\text{Si}$ ).

**Telechelic PDMS10K-TA:** The same procedure as for telechelic PDMS1K-TA was used, except that 24.57 g (2.80 mmol) PDMS10K-OMs was treated with 1.28 g (11.20 mmol) potassium thioacetate. A clear colourless viscous liquid was obtained after work-up. Yield: 23.92 g, 98%.  $^1\text{H NMR}$  (400 MHz,  $\text{CDCl}_3$ , ppm): 3.54 (t,  $\text{OCH}_2\text{CH}_2\text{SAC}$ ), 3.40 (t,  $\text{CH}_2\text{SAC}$ ), 3.09 (t,  $\text{CH}_2\text{OCH}_2\text{CH}_2\text{SAC}$ ), 2.33 (s,  $\text{SCOCH}_3$ ), 1.54–1.62 (m,  $\text{OCH}_2\text{CH}_2\text{CH}_2$ ), 0.49 – 0.53 (broad t,  $\text{CH}_2\text{Si}$ ), -0.08 – 0.22 (m,  $(\text{CH}_3)_2\text{Si}$ ).

**Synthesis of telechelic PDMS-SH:** **Telechelic PDMS1K-SH:** Into a three-necked round bottom flask equipped with condenser and gas inlet, a solution of 28.00 g (18.62 mmol) telechelic PDMS1K-TA in 30 mL anhydrous THF was charged under argon atmosphere. Subsequently, 22.00 g (372.30 mmol) n-propylamine was added using a syringe. The solution was refluxed at 40 °C under argon atmosphere overnight. When the mixture was cooled to room temperature, 40 mL dilute hydrochloric acid (10%) and brine (300 mL) were added under a steady stream of argon. The mixture was then extracted with diethyl ether ( $3 \times 100$  mL) and the combined organic layers were washed with brine ( $3 \times 200$  mL), dried over anhydrous  $\text{MgSO}_4$  and filtered over a celite 545 patch. After concentrating in vacuo, a clear slightly yellow viscous liquid was obtained and dried under vacuum at room temperature overnight. Yield: 26.09 g, 96%.  $^1\text{H NMR}$  (400 MHz,  $\text{CDCl}_3$ , ppm): 3.55 (t,  $\text{OCH}_2\text{CH}_2\text{SH}$ ), 3.40 (t,  $\text{CH}_2\text{OCH}_2\text{CH}_2\text{SH}$ ), 2.66 (q,  $\text{CH}_2\text{SH}$ ), 1.54–1.70 (m,  $\text{OCH}_2\text{CH}_2\text{CH}_2$  and  $\text{SH}$ ), 0.51 – 0.55 (broad t,  $\text{CH}_2\text{Si}$ ), -0.08 – 0.22 (m,  $(\text{CH}_3)_2\text{Si}$ ).

**Telechelic PDMS5K-SH:** The same procedure as for telechelic PDMS1K-SH was used, except that 22.89 g (4.74 mmol) telechelic PDMS5K-TA was treated with 5.56 g (94.72 mmol) n-propylamine. A clear slightly yellow viscous liquid was obtained after work-up. Yield: 21.83 g, 97%.  $^1\text{H NMR}$  (400 MHz,  $\text{CDCl}_3$ , ppm): 3.56 (t,  $\text{OCH}_2\text{CH}_2\text{SH}$ ), 3.40 (t,  $\text{CH}_2\text{OCH}_2\text{CH}_2\text{SH}$ ), 2.67 (q,  $\text{CH}_2\text{SH}$ ), 1.54–1.70 (m,  $\text{OCH}_2\text{CH}_2\text{CH}_2$  and  $\text{SH}$ ), 0.51 – 0.55 (broad t,  $\text{CH}_2\text{Si}$ ), -0.08 – 0.22 (m,  $(\text{CH}_3)_2\text{Si}$ ).

**Telechelic PDMS10K-SH:** The same procedure as for telechelic PDMS1K-SH was used, except that 22.74 g (2.6 mmol)



**Scheme 4.** Synthetic approach towards telechelic thiol-terminated PDMS oligomers. Three commercially available telechelic hydroxy-terminated PDMS oligomers with different molecular weights of approximately 1.0, 5.0 and 10  $\text{kg}\cdot\text{mol}^{-1}$  were used. The repeat unit ( $n$ ) of the polydimethylsiloxane equals 14, 68 and 135 for PDMS1K, 5K and 10K, respectively.

telechelic PDMS10K-TA was treated with 3.07 g (52 mmol) *n*-propylamine. A clear colorless viscous liquid was obtained after work-up. Yield: 21.46 g, 96%. <sup>1</sup>H NMR (400 MHz, CDCl<sub>3</sub>, ppm): 3.56 (t, OCH<sub>2</sub>CH<sub>2</sub>SH), 3.40 (t, CH<sub>2</sub>OCH<sub>2</sub>CH<sub>2</sub>SH), 2.67 (q, CH<sub>2</sub>SH), 1.54–1.70 (m, OCH<sub>2</sub>CH<sub>2</sub>CH<sub>2</sub> and SH), 0.51–0.55 (broad t, CH<sub>2</sub>Si), -0.08–0.22 (m, (CH<sub>3</sub>)<sub>2</sub>Si).

#### Synthesis of the AM- and LC- segmented block copolymers

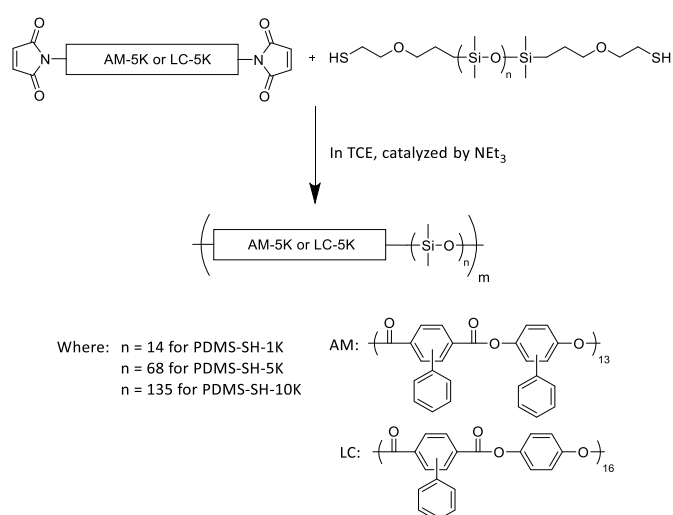
The all-aromatic AM oligomers with PDMS segments based segmented block copolymers were labelled, AM5K-*b*-PDMS1K, AM5K-*b*-PDMS5K and AM5K-*b*-PDMS10K, respectively, where AM5K-*b*-PDMS reflects the composition of the segmented block copolymer main-chain (A = the aromatic AM or LC block and B = the PDMS flexible block) and the integers refer to the molecular weight of the PDMS units, *i.e.* 1K = 1.0 kg·mol<sup>-1</sup>. A similar convention was applied to the segmented block copolymers composed of LC units and PDMS flexible blocks, labelled as LC5K-*b*-PDMS1K, LC5K-*b*-PDMS5K, LC5K-*b*-PDMS10K, respectively. The synthetic approach is shown in scheme 5.

**Optimization of synthetic conditions:** The observation of disulphide formation may prohibit a straightforward stoichiometric polymerisation, therefore the stoichiometry had to be optimized. A typical polymerization was performed with triethylamine (NEt<sub>3</sub>) as a catalyst under a dry nitrogen atmosphere.

**Synthesis of AM5K-*b*-PDMS:** *AM5K-*b*-PDMS1K:* Into a 250 mL three-necked flask equipped with an overhead mechanical stirrer and argon gas inlet, 3.68 g (0.75 mmol) AM5K and 36 mL TCE were charged under an argon atmosphere. Mechanical stirring at room temperature was applied until all the white solid dissolved, subsequently 1.04 g (0.71 mmol) PDMS1K-SH and 0.50 mL triethylamine was added. After evacuation and back filling with argon, the clear solution was stirred at 60 °C for 2 h. When the reaction mixture was cooled to room temperature, the viscous solution was precipitated in ethanol. The filtered white product was re-dissolved in dichloromethane (100 mL) and re-precipitated in ethanol (500 mL), which was repeated one more time. After drying under vacuum at 60 °C overnight, a white solid was obtained. Yield: 4.71 g (99%). <sup>1</sup>H NMR (400 MHz, CDCl<sub>3</sub>, ppm): 6.50–8.50 (aromatic), 4.05 (COCH<sub>3</sub>), 3.73 (SCH<sub>2</sub>CH<sub>2</sub>O), 3.43 (SCH<sub>2</sub>CH<sub>2</sub>OCH<sub>2</sub>CH<sub>2</sub>), 3.25 (SCH<sub>2</sub>CH<sub>2</sub>O), 2.72 and 2.97 (COCH<sub>2</sub>CHCO), 1.60 (OCH<sub>2</sub>CH<sub>2</sub>CH<sub>2</sub>), 0.53 (CH<sub>2</sub>Si), -0.07–0.22 ((CH<sub>3</sub>)<sub>2</sub>Si).

*AM5K-*b*-PDMS5K:* The same procedure as for AM5K-*b*-PDMS1K was used, except that 2.45 g (0.50 mmol) AM5K in 36 mL TCE was treated with 2.52 g (0.50 mmol) PDMS5K-SH and 0.5 mL NEt<sub>3</sub>. A white solid was obtained. Yield: 4.93 g (99%). <sup>1</sup>H NMR (400 MHz, CDCl<sub>3</sub>, ppm): 6.50–8.50 (aromatic), 4.03 (COCH<sub>3</sub>), 3.69 (SCH<sub>2</sub>CH<sub>2</sub>O), 3.43 (SCH<sub>2</sub>CH<sub>2</sub>OCH<sub>2</sub>CH<sub>2</sub>), 3.24 (SCH<sub>2</sub>CH<sub>2</sub>), 2.69 and 2.96 (COCH<sub>2</sub>CHCO), 1.62 (OCH<sub>2</sub>CH<sub>2</sub>CH<sub>2</sub>), 0.52 (CH<sub>2</sub>Si), -0.07–0.22 ((CH<sub>3</sub>)<sub>2</sub>Si).

*AM5K-*b*-PDMS10K:* The same procedure as for AM5K-*b*-PDMS1K was used, except that 1.96 g (0.40 mmol) AM5K in 36 mL TCE was treated with 4.63 g (0.40 mmol) PDMS10K-SH and 0.50 mL NEt<sub>3</sub>. A white solid was obtained. Yield: 6.55 g (99%). <sup>1</sup>H NMR (400 MHz, CDCl<sub>3</sub>, ppm): 6.50–8.50 (aromatic), 4.06 (COCH<sub>3</sub>), 3.73 (SCH<sub>2</sub>CH<sub>2</sub>O), 3.43 (SCH<sub>2</sub>CH<sub>2</sub>OCH<sub>2</sub>CH<sub>2</sub>), 3.24



**Scheme 5.** Synthetic route towards the (AB)<sub>*n*</sub>-multiblock copolymers from thiol-terminated PDMS oligomers and maleimide terminated AM or LC oligomers.

(SCH<sub>2</sub>CH<sub>2</sub>), 2.71 and 2.96 (COCH<sub>2</sub>CHCO), 1.61 (OCH<sub>2</sub>CH<sub>2</sub>CH<sub>2</sub>), 0.53 (CH<sub>2</sub>Si), -0.08–0.22 ((CH<sub>3</sub>)<sub>2</sub>Si).

**Synthesis of LC5K-*b*-PDMS:** Due to the limited solubility of the LC5K oligomer and the high molecular weight block copolymers thereof, the amount of solvent (TCE) and/or the final reaction temperature was adjusted in order to avoid premature precipitation and phase separation during synthesis.

*LC5K-*b*-PDMS1K:* Into a 250 mL three-necked flask equipped with an overhead mechanical stirrer and argon gas inlet, 3.73 g (0.70 mmol) LC5K and 36 mL TCE were charged under an argon atmosphere. The mixture was heated to 60 °C and stirred until all the white solid dissolved, subsequently 1.07 g (0.74 mmol) PDMS1K-SH and 0.50 mL triethylamine was added. After degassing and back filling with argon, the clear solution was stirred at 90 °C for 2 h. When the reaction mixture was cooled to room temperature, the viscous solution was precipitated in ethanol. The filtered white product was washed with hot dichloromethane and ethanol for two times. After drying under vacuum at 60 °C overnight, a white solid was obtained. Yield: 4.71 g (98%). <sup>1</sup>H NMR (400 MHz, CDCl<sub>3</sub> + TCE-*d*<sub>2</sub> 50/50, ppm): 6.50–8.60 (aromatic), 4.07 (COCH<sub>3</sub>), 3.70 (SCH<sub>2</sub>CH<sub>2</sub>O), 3.42 (SCH<sub>2</sub>CH<sub>2</sub>OCH<sub>2</sub>CH<sub>2</sub>), 3.20 (SCH<sub>2</sub>CH<sub>2</sub>), 2.70 and 2.95 (COCH<sub>2</sub>CHCO), 1.68 (OCH<sub>2</sub>CH<sub>2</sub>CH<sub>2</sub>), 0.52 (CH<sub>2</sub>Si), -0.09–0.21 ((CH<sub>3</sub>)<sub>2</sub>Si).

*LC5K-*b*-PDMS5K:* The same procedure as for LC5K-*b*-PDMS1K was used, except that 2.66 g (0.50 mmol) LC5K in 60 mL TCE was treated with 1.01 g (0.50 mmol) PDMS5K-SH and 0.50 mL NEt<sub>3</sub>. A white solid was obtained. Yield: 3.60 g (98%). <sup>1</sup>H NMR (400 MHz, CDCl<sub>3</sub> + TCE-*d*<sub>2</sub> 50/50, ppm): 6.50–8.60 (aromatic), 4.07 (COCH<sub>3</sub>), 3.70 (SCH<sub>2</sub>CH<sub>2</sub>O), 3.42 (SCH<sub>2</sub>CH<sub>2</sub>OCH<sub>2</sub>CH<sub>2</sub>), 3.21 (SCH<sub>2</sub>CH<sub>2</sub>), 2.70 and 2.96 (COCH<sub>2</sub>CHCO), 1.62 (OCH<sub>2</sub>CH<sub>2</sub>CH<sub>2</sub>), 0.51 (CH<sub>2</sub>Si), -0.09–0.20 ((CH<sub>3</sub>)<sub>2</sub>Si).

*LC5K-*b*-PDMS10K:* The same procedure as for LC5K-*b*-PDMS1K was used, except that 1.60 g (0.30 mmol) LC5K in 60 mL TCE was treated with 3.47 g (0.30 mmol) PDMS10K-SH and

0.50 mL NEt<sub>3</sub>. A white solid was obtained. Yield: 5.01 g (99%). <sup>1</sup>H NMR (400 MHz, CDCl<sub>3</sub> + TCE-*d*<sub>2</sub> 50/50, ppm): 6.50 – 8.60 (aromatic), 4.07 (COCH<sub>3</sub>), 3.70 (SCH<sub>2</sub>CH<sub>2</sub>O), 3.42 (SCH<sub>2</sub>CH<sub>2</sub>OCH<sub>2</sub>CH<sub>2</sub>), 3.21 (SCH<sub>2</sub>CH<sub>2</sub>), 2.70 and 2.97 (COCH<sub>2</sub>CHCO), 1.67 (OCH<sub>2</sub>CH<sub>2</sub>CH<sub>2</sub>), 0.52 (CH<sub>2</sub>Si), -0.09 – 0.21 ((CH<sub>3</sub>)<sub>2</sub>Si).

#### Characterization

**Nuclear magnetic resonance (NMR):** <sup>1</sup>H and <sup>13</sup>C nuclear magnetic resonance (NMR) spectra were recorded on a 400 MHz Agilent-400 MR DD2 at room temperature. All samples were dissolved in deuterated solvents and the recorded spectra were referenced to the solvent or to TMS (DMSO-*d*<sub>6</sub>: <sup>1</sup>H, 2.50 ppm and <sup>13</sup>C, 39.52 ppm, CDCl<sub>3</sub>: <sup>1</sup>H, 7.24 ppm and <sup>13</sup>C, 77.0 ppm, TCE-*d*<sub>2</sub>: <sup>1</sup>H, 6.00 ppm and <sup>13</sup>C, 73.78 ppm, TFA-*d*: <sup>1</sup>H, 11.50 ppm). Quantitative <sup>13</sup>C NMR spectra for end-group analysis were also recorded on a 400 MHz Agilent-400 MR DD2 spectrometer. A frequency of 100 MHz of inverse gated proton and long delays of 20 s between pulses and 1000 scans was used. All samples were dissolved in deuterated TCE and the recorded spectra were referenced to the solvent (TCE-*d*<sub>2</sub>: <sup>13</sup>C, 73.78 ppm).

**Gas chromatography–mass spectrometry (GC-MS):** GC-MS analyses were performed on a Shimadzu GC2010 series GC coupled to a MS detector (Shimadzu QP2010S), equipped with a BPX5 capillary column. The oven was heated from 50–300 °C at a rate of 10 °C·min<sup>-1</sup> using a 1 mL·min<sup>-1</sup> helium gas flow. The sample was injected using an ATAS GL Optic 3 inlet which was heated from 50–300 °C in one minute. Mass spectra were generated by electron impact and data was collected over the *m/z* range 45–900. Mass spectra were recorded using a Shimadzu QP2010S with direct injection port.

**Fourier transform infrared spectroscopy (FTIR):** FTIR spectra were recorded using a Perkin Elmer Spectrum 100 FTIR spectrometer.

**Gel permeation chromatography (GPC):** The molecular weight distributions of the AM5K oligomer were determined using GPC. Samples were prepared at tetrahydrofuran (THF) and filtered through a 0.45 μm PTFE syringe filter. Measurements were performed using a Shimadzu GPU DGU-20A3, equipped with a Shodex LF-801 column and refractive index detector. THF was used as the eluent at a flow rate of 0.5 mL·min<sup>-1</sup> at 60 °C. For the GPC measurement of segmented block copolymers, THF was used as the eluent at a flow rate of 1.0 mL·min<sup>-1</sup> and at a temperature of 40 °C. Molecular weights were calculated using a polystyrene standard calibration curve and data analyses were performed using labSolutions software from the refractive index detector data. All polymers and oligomers were filtered through a 0.45 μm PTFE filter prior to a GPC run.

**Viscometry:** An Ubbelohde viscometer was used to measure the flow time of pure solvent and polymer or oligomer solutions. All viscosity measurements were carried out at 21 ± 0.01 °C in a water bath equipped with an automatic temperature controller. The flow time of pure solvent in the viscometer was first recorded. Afterwards, the flow time of an oligomer or polymer solution with known concentration (0.5 g·dL<sup>-1</sup>) was measured. The ratio of flow time of polymer solution to that of pure solvent is regarded as the relative viscosity ( $\eta_{rel}$ ).

Therefore, the specific viscosity ( $\eta_{sp}$ ) is defined as an increment of relative viscosity, and can be calculated using equation 1.

$$\eta_{sp} = \eta_{rel} - 1 \quad (\text{eqn. 1})$$

The inherent viscosity ( $\eta_{inh}$ ) was calculated according to equation 2, where *c* is the concentration of the polymer solution (g·dL<sup>-1</sup>).

$$\eta_{inh} = \frac{\ln \eta_{rel}}{c} \quad (\text{eqn. 2})$$

Solomon and Ciută reported the determination of intrinsic viscosity from one viscosity measurement of a polymer solution, using equation 3.<sup>56, 57</sup>

$$[\eta] = \frac{\sqrt{2}}{c} \times \sqrt{\eta_{sp} - \ln \eta_r} \quad (\text{eqn. 3})$$

The Mark-Houwink-Sakurada equation relates the intrinsic viscosity ( $[\eta]$ ) to the number average molecular weight (*M*).

$$[\eta] = K \times M^\alpha \quad (\text{eqn. 4})$$

For poly(*p*-phenylene phenyl terephthalate) (*i.e.* LC5K), the values of *K* and  $\alpha$  were reported to be 1.06×10<sup>-2</sup> and 1.0, respectively.<sup>58</sup> The *K* and  $\alpha$  values at a low molecular weight range (25 ≤  $[\eta]$  ≤ 257 cm<sup>3</sup>·g<sup>-1</sup>) for poly(phenyl-*p*-phenylene phenyl terephthalate) (*i.e.* AM5K) were calculated to be 4.00×10<sup>-3</sup> and 1.11, respectively.<sup>59</sup>

**Thermogravimetric analysis (TGA):** A Perkin Elmer Pyris Diamond TG/DTA was used to study the dynamic thermal stability. The samples were analyzed using a heating rate of 10 °C·min<sup>-1</sup> under a nitrogen atmosphere.

**Differential scanning calorimetry (DSC):** The transition temperatures of the block copolymers were determined by DSC using a Perkin Elmer DSC 8000 with a heating rate of 40 °C·min<sup>-1</sup> under a helium gas atmosphere.

**Dynamic mechanical thermal analyses (DMTA):** DMTA was performed using a Perkin Elmer Diamond DMTA in tension mode, using thin films of the following approximate dimensions: 20 × 4 × 0.1 mm<sup>3</sup>. All experiments were performed under a nitrogen atmosphere and at a heating rate of 2 °C·min<sup>-1</sup> at a frequency of 1 Hz.

**Transmission electron microscopy (TEM):** Transmission electron microscopy (TEM) was performed using a Jeol 100CX and operating at 80 kV at room temperature. All of the samples were prepared by cryo-microtome using a Leica UT7/UTC at -80 °C and transferred onto a copper grid.

AFM: Atomic force microscopy (AFM) topological and phase angle maps were obtained with an Asylum Research MFP3D Atomic Force Microscope. A scan rate of 0.50 Hz was utilized to scan a size of 5 μm × 5 μm. The images shown are from cross-sections of the films; samples were cut using a sharp razor and mounted on to a clean glass plate using copper tape such that the cross-section could be mapped using an AFM. Images were obtained approximately in the centre of the cross-section.

**Dual shape memory test:** The dual shape memory test was performed on a Thermofisher Haake MARS III rheometer equipped with solid clamp geometry with rectangular thin films (approximately 25 × 5 × 0.2 mm<sup>3</sup>) in controlled torsion mode. All tests were carried out under an air atmosphere and at a constant strain rate of 0.1%·s<sup>-1</sup>, equivalent to a rotation speed of 3 °·s<sup>-1</sup>. The heating and cooling rates are 10 °C·min<sup>-1</sup>.

Generally, the experiment was conducted by a rotation of 180° and the recovery under stress-free condition was

measured. The film was first kept at 150 °C for 10 min, which is well above  $T_g$  of the aromatic segments, and rotated by 180° from the original shape to a temporary deformed shape ( $\varphi_d$ ). After a 10 min hold at this temperature, the sample was cooled to 20 °C at a cooling rate of 10 °C·min<sup>-1</sup>, to fix the temporary shape. To quantify the shape memory effect, shape fixation rate ( $R_f$ ) is defined as

$$R_f = \frac{\varphi_f}{\varphi_d} \times 100\% \quad (\text{eqn. 5})^{50}$$

and the shape recovery rate ( $R_r$ ) is given by

$$R_r = \frac{\varphi_d - \varphi_r}{\varphi_d} \times 100\% \quad (\text{eqn. 6})^{50}$$

Where  $\varphi_d$ ,  $\varphi_f$  and  $\varphi_r$  stand for the rotational angle after deformation, at the fixed temporary shape and after recovery, respectively.  $R_f$  and  $R_r$  are the percentage of shape fixation and shape recovery, respectively. The instantaneous recovery velocity  $V_r$  is defined as the time derivative of the angle as shown in Equation 7, to clarify the recovery temperature range corresponding to the shape recovery process.

$$V_r = \frac{\partial \varphi}{\partial t} \quad (\text{eqn. 7})^{50}$$

**Triple shape memory test:** The triple shape memory test was also performed on a Thermofisher Haake MARS III rheometer equipped with solid clamp geometry with rectangular thin films in controlled torsion mode with the film dimensions of approximately 25 × 5 × 0.2 mm<sup>3</sup>. The constant strain rate and the heating/cooling rate used for the test are

described above. The triple torsion SMP experiment was conducted following the protocols shown in Figure 10.

Generally, the experiment was conducted by two rotation steps (e.g., 90° + 90°), to a constant total rotation of 180°. The sample was kept isothermal at 150 °C, which is well above  $T_g$  of the aromatic units, and rotated by 90° from the original shape A ( $\varphi_A$ ) to a temporary shape B ( $\varphi_B$ ). After holding at temperature for 10 min, the sample was cooled to 20 °C, which is between the two glass transition temperatures. After stabilizing at this temperature for 10 min, a second stress was applied to rotate the sample to another temporary shape C ( $\varphi_C$ ). The sample was subsequently cooled to -150 °C, which is well below the  $T_g$  of the PDMS units, to fix a temporary shape C. During this two-step programming process, measuring the rotation degree  $\varphi_C$  and the final fixed rotation degree  $\varphi_f$ , the shape fixation rate ( $R_f$ ) can be defined as

$$R_f = \frac{\varphi_f}{\varphi_C} \times 100\% \quad (\text{eqn. 8})^{50}$$

In the subsequent recovery step, the sample was allowed to recover upon heating with the release of external stress. The two-step recovery rates ( $R_r$ ) can be calculated using the following equations:

$$R_{r(C \rightarrow B)} = \frac{\varphi_f - \varphi_{B/rec}}{\varphi_C - \varphi_B} \times 100\% \quad (\text{eqn. 9})^{50}$$

$$R_{r(B \rightarrow A)} = \frac{\varphi_{B/rec} - \varphi_{A/rec}}{\varphi_B - \varphi_A} \times 100\% \quad (\text{eqn. 10})^{50}$$

Where  $\varphi_A$ ,  $\varphi_B$  and  $\varphi_C$  denote the degree of rotation after the torsion step, the degree of rotation of the fixed temporary shape, and the degree of rotation after recovery, respectively.

## Conclusions

We have prepared two series high molecular weight segmented block copolymers by reacting all-aromatic liquid crystal (LC) and amorphous (AM) telechelic ester-based maleimide-functionalized oligomers ( $M_n = 5 \text{ kg}\cdot\text{mol}^{-1}$ ) with telechelic thiol-terminated poly(dimethylsiloxane)s (PDMS,  $M_n = 1, 5$  and 10  $\text{kg}\cdot\text{mol}^{-1}$ ). <sup>1</sup>H NMR measurements confirmed that the block copolymers exhibit high molecular weights with  $M_n$ s in the range of 22–58  $\text{kg}\cdot\text{mol}^{-1}$ . The AM5K-*b*-PDMS multiblock copolymers are amorphous whereas the LC5K-*b*-PDMS multiblock copolymers retain their liquid crystallinity even with a concentration of LC segments as low as 30 wt%. DSC and DMTA experiments confirmed that the multiblock copolymers with 5K and 10K PDMS segments show two glass transition events, indicating the presence of micro-phase separated domains. This is due to the incompatibility of the rigid aromatic ester blocks and flexible PDMS blocks. However, as a result of the high polydispersity, phase separation is difficult to observe by TEM. During tensile testing, the AM5K-*b*-PDMS multiblock copolymers show excellent mechanical stress-strain behavior. The AM5K-*b*-PDMS1K film shows a tensile strength of 125 MPa, an elastic modulus of 3.4 GPa and elongation at break >30%. Films prepared from LC5K blocks, on the other hand, show inferior stress-strain behavior, which is believed to be the direct result of the incompatibility of the LC5K block and the PDMS block.

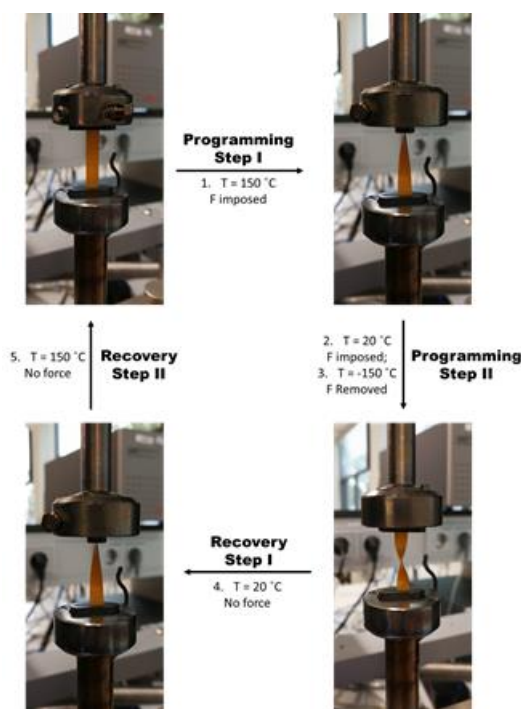


**Fig. 10.** Illustration of the triple-SMP experiment performed using a rheometer in controlled torsion mode. Samples were tested between -150 to 150 °C and twisted 90° and 180°. Dual-SMP experiment was performed in a similar fashion, between 20 to 150 °C and twisted 180°. Comparing to characterization under tension mode, with this set-up, samples are able to be exposed the large deformations but they experience little strain.

The dual- and triple-shape fixation and recovery performance of free-standing films was investigated in torsion mode. The AM5K- and LC5K-b-PDMS1K multiblock copolymers show high temperature dual-shape memory behavior ( $>150\text{ }^{\circ}\text{C}$ ) by using the  $T_g$ s of the rigid segments as the thermal triggers. The AM5K-b-PDMS1K block copolymer shows high  $R_f$  (100%) and  $R_r$  ( $>97\%$ ) values, whereas LC5K-b-PDMS1K exhibits moderate shape memory performance, with an  $R_f$  of 97% and  $R_r > 80\%$ . The PDMS5K-based multiblock copolymers show triple-SME when using the two  $T_g$ s as temperature switches. High  $R_f$  ( $>95\%$ ) and high  $R_r$  ( $>96\%$ ) values were measured for AM5K-b-PDMS5K, whereas LC5K-b-PDMS5K exhibits slightly lower  $R_f$  values of  $>91\%$  and  $R_r > 80\%$ , respectively. The combination of excellent mechanical performance and shape memory properties of the AM5K-PDMS segmented block copolymer series enables the design of structural materials that can be programmed with a shape-memory function over a broad temperature range.

### Conflicts of interest

There are no conflicts to declare.

### Acknowledgements

Hongli Xu gratefully acknowledges in-part funding from the Chinese Scholarship Council (#201206340070). We would like to thank Dr. Wallace Ambrose (UNC Chapel Hill) and Dr. Wiel Evers (TNW, TU-Delft) for their help with the cryo-TEM experiments. We acknowledge Dr. Amar Kumbhar for performing the AFM work. This was performed at the Chapel Hill Analytical and Nanofabrication Laboratory (CHANL), member of the North Carolina Research Triangle Nanotechnology Network (RTNN) which is supported by the National Science Foundation, Grant ECCS-1542015, as part of the National Nanotechnology Coordinated Infrastructure (NNCI).

### Notes and references

- N. Hadjichristidis, S. Pispas and G. Floudas, in *Block Copolymers*, John Wiley & Sons, Inc., 2003, DOI: 10.1002/0471269808.ch21, pp. 383-408.
- S. Fakirov, *Handbook of Condensation Thermoplastic Elastomers*, Wiley, 2006.
- D. Pospiech, L. Häußler, K. Eckstein, H. Komber, D. Voigt, D. Jehnichen, P. Friedel, A. Gottwald, W. Kollig and H. R. Kricheldorf, *High Perform. Polym.*, 2001, **13**, S275-S292.
- J.-C. Ho, Y.-S. Lin and K.-H. Wei, *Polymer*, 1999, **40**, 3843-3853.
- Y. Oishi, S. Nakata, M. A. Kakimoto and Y. Imai, *J. Polym. Sci., Part A: Polym. Chem.*, 1993, **31**, 1111-1117.
- V. Percec and B. C. Auman, *Makromol. Chem.*, 1984, **185**, 617-627.
- V. Percec and B. C. Auman, *Polym. Bull.*, 1984, **12**, 253-260.
- T. D. Shaffer and V. Percec, *Makromol. Chem.*, 1986, **187**, 111-123.
- K. Mitrach, D. Pospiech, L. Häußler, D. Voigt, D. Jehnichen and M. Rätzsch, *Polymer*, 1993, **34**, 3469-3474.
- J. E. McGrath, D. L. Dunson, S. J. Mecham and J. L. Hedrick, in *Progress in Polyimide Chemistry I*, ed. H. R. Kricheldorf, Springer Berlin Heidelberg, Berlin, Heidelberg, 1999, pp. 61-105.
- C. M. Mahoney, J. A. Gardella and J. C. Rosenfeld, *Macromolecules*, 2002, **35**, 5256-5266.
- A. Ghosh and S. Banerjee, *Polym. Adv. Technol.*, 2008, **19**, 1486-1494.
- A. Ghosh, S. K. Sen, S. Banerjee and B. Voit, *RSC Adv.*, 2012, **2**, 5900-5926.
- A. Ghosh and S. Banerjee, *J. Appl. Polym. Sci.*, 2008, **109**, 2329-2340.
- C.-K. Ku and Y.-D. Lee, *Polymer*, 2007, **48**, 3565-3573.
- S. Andre, F. Guida-Pietrasanta, A. Rousseau and B. Boutevin, *J. Polym. Sci., Part A: Polym. Chem.*, 2001, **39**, 2414-2425.
- C. A. Arnold, D. H. Chen, Y. P. Chen, R. O. Waldbauer, M. E. Rogers and J. E. McGrath, *High Perform. Polym.*, 1990, **2**, 83-94.
- M. Kajiyama, M. Kakimoto and Y. Imai, *Macromolecules*, 1989, **22**, 4143-4147.
- L. T. Cureton, F. L. Beyer and S. R. Turner, *Polymer*, 2010, **51**, 1679-1686.
- D. P. Nair, M. Podgórski, S. Chatani, T. Gong, W. Xi, C. R. Fenoli and C. N. Bowman, *Chem. Mater.*, 2014, **26**, 724-744.
- A. B. Lowe, *Polym. Chem.*, 2010, **1**, 17-36.
- I. A. Mohammed and A. Mustapha, *Molecules*, 2010, **15**, 7498.
- P. S. G. Krishnan, C. He and C. T. S. Shang, *J. Polym. Sci., Part A: Polym. Chem.*, 2004, **42**, 4036-4046.
- J. O. Park and S. H. Jang, *J. Polym. Sci., Part A: Polym. Chem.*, 1992, **30**, 723-729.
- G. Pitchaimari and C. T. Vijayakumar, *J. Appl. Polym. Sci.*, 2014, **131**, 39935.
- H. T. Land, W. Hatke, A. Greiner, H.-W. Schmidt and W. Heitz, *Makromol. Chem.*, 1990, **191**, 2005-2016.
- N. Miyaura, T. Yanagi and A. Suzuki, *Synth. Commun.*, 1981, **11**, 513-519.
- N. Reichelt, U. Schulze and H.-W. Schmidt, *Macromol. Chem. Phys.*, 1997, **198**, 3907-3930.
- U. Schulze and H.-W. Schmidt, *Polym. Bull.*, 1998, **40**, 159-166.
- O. van den Berg, L.-T. T. Nguyen, R. F. A. Teixeira, F. Goethals, C. Özdilek, S. Berghmans and F. E. Du Prez, *Macromolecules*, 2014, **47**, 1292-1300.
- L. Feng, H. Fang, S. Zhou and L. Wu, *Macromol. Chem. Phys.*, 2006, **207**, 1575-1583.
- W. R. Krigbaum, H. Hakemi and R. Kotek, *Macromolecules*, 1985, **18**, 965-973.
- Yi, X. Fan, X. Wan, L. Li, N. Zhao, X. Chen, J. Xu and Q.-F. Zhou, *Macromolecules*, 2004, **37**, 7610-7618.
- G. Liu, W.-S. Hung, J. Shen, Q. Li, Y.-H. Huang, W. Jin, K.-R. Lee and J.-Y. Lai, *Journal of Materials Chemistry A*, 2015, **3**, 4510-4521.
- S. N. Chvalun, M. Ishaq, J. Blackwell and A. Y. Bilibin, *Journal of Macromolecular Science, Part B*, 1998, **37**, 451-462.
- X. Chen, J. A. Gardella and P. L. Kumler, *Macromolecules*, 1992, **25**, 6631-6637.
- Des. Monomers. Polym.*, 1998, **1**, 103-109.
- Des. Monomers. Polym.*, 1998, **1**, 187-206.
- E.-C. Kang, T. Kaneko, D. Shiino and M. Akashi, *J. Polym. Sci., Part A: Polym. Chem.*, 2003, **41**, 841-852.
- T. Otsuki, M.-A. Kakimoto and Y. Imai, *J. Polym. Sci., Part A: Polym. Chem.*, 1991, **29**, 611-618.



41. Y. Imai, M. Kajiyama, S.-i. Ogata and M.-a. Kakimoto, *Polym. J.*, 1984, **16**, 267-272.
42. S. Ogata, M. Kakimoto and Y. Imai, *Macromolecules*, 1985, **18**, 851-855.
43. L. Leibler, *Macromolecules*, 1980, **13**, 1602-1617.
44. P. Thorsten, *Smart Mater. Struct.*, 2010, **19**, 015006.
45. X. Luo, X. Zhang, M. Wang, D. Ma, M. Xu and F. Li, *J. Appl. Polym. Sci.*, 1997, **64**, 2433-2440.
46. G. Rabani, H. Luftmann and A. Kraft, *Polymer*, 2006, **47**, 4251-4260.
47. H. Y. Lee, H. M. Jeong, J. S. Lee and B. K. Kim, *Polym. J.*, 2000, **32**, 23.
48. W. Wagermaier, K. Kratz, M. Heuchel and A. Lendlein, in *Shape-Memory Polymers*, ed. A. Lendlein, Springer Berlin Heidelberg, Berlin, Heidelberg, 2010, DOI: 10.1007/12\_2009\_25, pp. 97-145.
49. J. Diani, C. Frédy, P. Gilormini, Y. Merckel, G. Régnier and I. Rousseau, *Polym. Test.*, 2011, **30**, 335-341.
50. Q. Guan, S. J. Picken, S. S. Sheiko and T. J. Dingemans, *Macromolecules*, 2017, **50**, 3903-3910.
51. C. Liu, H. Qin and P. T. Mather, *J. Mater. Chem.*, 2007, **17**, 1543-1558.
52. R. A. Weiss, E. Izzo and S. Mandelbaum, *Macromolecules*, 2008, **41**, 2978-2980.
53. Q. Wang, Y. Bai, Y. Chen, J. Ju, F. Zheng and T. Wang, *J. Mater. Chem. A*, 2015, **3**, 352-359.
54. Q. Zhao, H. J. Qi and T. Xie, *Prog. Polym. Sci.*, 2015, **49**, 79-120.
55. M. Behl and A. Lendlein, *Mater. Today*, 2007, **10**, 20-28.
56. O. F. Solomon and I. Z. Ciută, *J. Appl. Polym. Sci.*, 1962, **6**, 683-686.
57. V. O. F. Solomon and B. S. Gotesman, *Makromol. Chem.*, 1967, **104**, 177-184.
58. V. N. Tsvetkov, S. V. Bushin, L. N. Andreeva, C. P. Smirnov, E. V. Belyaeva, A. Y. Bilibin and A. R. Stepanova, *Eur. Polym. J.*, 1992, **28**, 91-96.
59. S. V. Bushin, K. P. Smirnov, L. N. Andreeva, Y. V. Belyaeva, A. Y. Bilibin, A. R. Stepanova and V. N. Tsvetkov, *Polym. Sci. (USSR) (Engl. Transl.)*, 1990, **32**, 1015-1021.

Aromatic-PDMS (AB)<sub>n</sub> multiblock copolymers: A one-component polymeric system that combines excellent mechanical properties with shape memory capability.

